Published in final edited form as:
Brain Struct Funct. 2013 March ; 218(2): 455–475. doi:10.1007/s00429-012-0408-3.

Cholinergic neurons in the mouse rostral ventrolateral medulla target sensory afferent areas

Ruth L. Stornetta, **Conrad J. Macon**, **Thanh M. Nguyen**, **Melissa B. Coates**, and **Patrice G. Guyenet**
Department of Pharmacology, University of Virginia, Charlottesville, VA 22908

Abstract

The rostral ventrolateral medulla (RVLM) primarily regulates respiration and the autonomic nervous system. Its medial portion (mRVLM) contains many choline acetyltransferase (ChAT)-immunoreactive (ir) neurons of unknown function. We sought to clarify the role of these cholinergic cells by tracing their axonal projections. We first established that these neurons are neither parasympathetic preganglionic neurons nor motor neurons because they did not accumulate intraperitoneally administered Fluorogold. We traced their axonal projections by injecting a Cre-dependent vector (floxed-AAV2) expressing either GFP or mCherrry into the mRVLM of ChAT-Cre mice. Transduced neurons expressing GFP or mCherry were confined to the injection site and were exclusively ChAT-ir. Their axonal projections included the dorsal column nuclei, medullary trigeminal complex, cochlear nuclei, superior olivary complex and spinal cord lamina III. For control experiments, the floxed-AAV2 (mCherry) was injected into the RVLM of dopamine beta-hydroxylase-Cre mice. In these mice mCherry was exclusively expressed by RVLM catecholaminergic neurons. Consistent with data from rats, these catecholaminergic neurons targeted brain regions involved in autonomic and endocrine regulation. These regions were almost totally different from those innervated by the intermingled mRVLM-ChAT neurons.

This study emphasizes the advantages of using Cre-driver mouse strains in combination with floxed-AAV2 to trace the axonal projections of chemically defined neuronal groups. Using this technique, we revealed previously unknown projections of mRVLM-ChAT neurons and showed that despite their close proximity to the cardiorespiratory region of the RVLM, these cholinergic neurons regulate sensory afferent information selectively and presumably have little to do with respiration or circulatory control.

Keywords

medulla oblongata; acetylcholine; somatosensory processing

Introduction

The rostral ventrolateral medulla oblongata (RVLM) contains an incompletely characterized network of neurons that regulate respiration and blood pressure (Guyenet 2006; Smith et al. 2009; Feldman et al. 2009) in addition to adrenaline release, cerebral blood flow, arousal, the CRF-ACTH-corticosterone cascade and glucoprivic feeding (Ennis et al. 1992; Golanov et al. 2000; Sawchenko et al. 2000; Li et al. 2009). The medial aspect of the rat RVLM harbors neurons of unknown function which are immunoreactive for choline

Address correspondence to: Ruth L. Stornetta, PhD, University of Virginia Health System, P.O. Box 800735, 1300 Jefferson Park Avenue, Charlottesville, VA 22908-0735. Tel: (434) 982-3977; Fax: (434) 982-3878; rs3j@virginia.edu.

acetyltransferase (ChAT) (Ruggiero et al. 1990). In the rat, these neurons (henceforth called mRVLM-ChAT neurons) form a longitudinally oriented column that extends lateral to the pyramidal tract from the caudal end of the facial motor nucleus to the level of the area postrema (Ruggiero et al., 1990). They are small, contain lower levels of ChAT immunoreactivity than nearby motor neurons and have often been overlooked (Ichikawa et al. 1997). Padley et al. (2007) could not detect the presence of vesicular acetylcholine transporter (VAChT) in the somata of these ChAT-ir neurons and therefore questioned their cholinergic nature. Yet, according to the Allen Mouse Brain Atlas (Allen Mouse Brain Atlas [Internet], 2009), the very same region of the mouse medulla oblongata harbors neurons that contain low but nonetheless clearly detectable levels of mRNA transcripts for ChAT, vesicular acetylcholine (ACh) transporter (VAChT, Slc18a3, solute carrier family 18 (vesicular monoamine), member 3) (Chaudhry et al. 2008) and choline transporter (CHT1, Slc5a7, solute carrier family 5 (choline transporter), member 7) (Okuda et al. 2000). Since both VAChT and CHT1 are selectively expressed by cholinergic neurons, these findings suggest that the mRVLM-ChAT neurons are indeed cholinergic neurons.

Our first objective was to ascertain that the mRVLM-ChAT neurons are neither parasympathetic preganglionic neurons nor motor neurons since the presence of such neurons within the RVLM and their role in airway control and cardiopulmonary regulation are well established (Bieger and Hopkins 1987; Standish et al. 1995). This was done by testing whether the mRVLM-ChAT neurons accumulate Fluorogold after intraperitoneal administration. Fluorogold is a retrogradely transported dye that, when injected intraperitoneally, only labels CNS neurons that have processes outside the blood brain barrier (Leong and Ling 1990).

Our second objective was to determine whether the mRVLM-ChAT neurons are a component of the network that regulates cardiorespiratory function. This hypothesis is supported by the argument of proximity since these ChAT cells are to a large extent co-mingled with the C1 adrenergic neurons and are relatively close to the Bötzinger / preBötzinger subdivisions of the respiratory network (Guyenet, 2006; Alheid and McCrimmon 2008). The hypothesis also derives some plausibility from the fact that the activity of the cardiorespiratory network is strongly stimulated by acetylcholine (Punnen et al. 1986; Giuliano et al. 1989; Huangfu et al. 1997; Shao et al. 2008).

However, the location of the mRVLM-ChAT neurons is also reminiscent of a group of neurons of undefined transmitter phenotype that innervate the dorsal column nuclei in cats (Kamiya et al. 1988). Supporting this hypothesis, in the rat, a few ChAT-ir neurons located in what appears to be the mRVLM as presently defined were retrogradely labeled after injection of cholera toxin B into the gracile nucleus (Fernandez de Sevilla et al. 2006). The mRVLM-ChAT neurons could therefore be regulating sensory perception rather than respiration, blood pressure or miscellaneous visceral organs.

In order to address this question, we mapped the axonal projections of the mRVLM-ChAT neurons and compared them with those of the neighboring C1 neurons which, in rats, target a well-defined set of structures involved in cardiorespiratory and autonomic regulations (Guyenet, 2006; Card et al. 2006). The projections of the mRVLM-ChAT neurons were examined by injecting a floxed adeno-associated viral vector (AAV) into the brain of a transgenic strain of mice that expresses Cre recombinase under the control of the ChAT promoter (ChAT-Cre mice (Lowell et al. 2006)). We selected for these experiments a serotype-2 AAV that remained narrowly confined to the injection site and did not infect neurons retrogradely. In control experiments we traced the projections of the co-mingled C1 neurons by injecting the same vector into the RVLM of mice expressing Cre recombinase

under the control of dopamine beta-hydroxylase (DBH), an enzyme present exclusively in noradrenergic and adrenergic neurons.

With this method we succeeded in transducing a single class of RVLM neurons in each of the two mouse strains with apparently complete selectivity and we showed that, despite the proximity of their cell bodies, the catecholaminergic and the cholinergic neurons of the RVLM target entirely different brain regions. Based on their projection patterns, the mRVLM-ChAT neurons appear to regulate incoming somatosensory information selectively and probably have little to do with cardiorespiratory control.

Materials and Methods

Animals

The experiments were performed in two strains of adult mice of mixed sex, in accordance with NIH and Institutional Animal Care and Use Guidelines. The Animal Research Committee of the University of Virginia approved all procedures and protocols. ChAT-Cre mice (strain B6;129S6-*Chattm1(cre)Lowl*/J) developed by Dr. B. Lowell, Beth Israel Deaconess Medical Center, Boston, MA were obtained from Jackson Labs, Bar Harbor, ME. DBH-Cre mice (strain STOCK Tg(Dbh-cre)KH212Gsat/Mmcd) developed by Dr. N. Heintz, Rockefeller University through the GENSAT project (Gong et al. 2003) were procured from the Mutant Mouse Regional Resource Centers.

Surgery and injections

Fluorogold injections—Fluorogold (FG, 1% in sterile water) was injected intraperitoneally (200 μl) in 4 adult (25-35 g) ChAT-Cre mice (2 females and 2 males). FG is excluded from the blood brain barrier. Therefore when injected peripherally, this compound only labels neurons with axons that exit the brain and neurons that reside within the circumventricular organs (Leong and Ling, 1990). After survival for 10-14 days, animals were deeply anesthetized with pentobarbital and perfused transcardially as described below.

Virus injections—Adult ChAT-Cre or DBH-Cre mice (25-35 g), of either sex were anesthetized with a mixture of ketamine and xylazine (100 and 10 mg/kg, respectively) injected i.p or with a mixture of ketamine and dexdemetomidine given i.p. (100 mg/kg and 0.2 mg/kg, respectively). The mice were placed on a stereotaxic apparatus with the bite bar set 2.0 mm below the ear bars and were maintained at 36-37 °C with a servo-controlled heating pad. A 1.5 cm incision was made in the skin over the skull and a 1.5 mm diameter burr hole drilled through the occipital plate to inject one of two AAVs into the RVLM. In half of the ChAT-Cre and all the DBH-Cre mice we injected double-floxed inverted open reading frame ChannelRhodopsin2-mCherry AAV2 (AAV2-floxed-ChR2-mCherry). This vector expresses the fusion protein ChR2-mCherry under the control of the eF1α promoter (Cardin et al. 2009). The construct was kindly provided by Dr. K. Deisseroth, Stanford University, and the AAV was produced as a serotype 2 by the University of North Carolina Vector core (Chapel Hill, NC; titer: 10^{12} virus molecules per ml). In the rest of the ChAT-Cre mice we used AAV-MCS8 loxP_neo_loxP_hrGFP serotype 2 (AAV2-floxed-GFP) (Gautron et al. 2010), a generous gift of Dr. C.B. Saper (Beth Israel Deaconess Medical Center, Boston, MA). The viral vectors were injected through a glass pipette pulled to a 25 micron outside diameter at the tip, which was connected to an electronically controlled pressure valve (Picospritzer). The pipette was used first to locate the facial motor nucleus by recording antidromic field potentials elicited by electrical stimulation of the mandibular branch of the facial nerve (0.1 ms, 0.1-1 mA). Once the facial field was located the pipette tip was moved medial to the caudal and lower edge of the facial motor nucleus or slightly caudal to that site. The stereotaxic coordinates selected to target the region containing the

mRVLM ChAT neurons were approximately 0.7 mm lateral to midline, 1.2 mm caudal to lambda and 6 mm ventral to the cerebellar surface with individual adjustments of up to 300 microns in all directions depending on the electrophysiologically identified location of the facial motor nucleus. The coordinates used to target the catecholaminergic neurons of the RVLM were on average 1.1 mm lateral, 1.3 mm caudal, 5.6 mm below the cerebellar surface. Short air pressure pulses (3-6 ms) were used to inject a total of 200-300 nl of vector over 10 minutes into two locations in ChAT-Cre mice or three locations in DBH-Cre mice at 200 micron intervals and aligned along the rostrocaudal axis of the animal. The pipette was then removed, the incision washed and the wound closed with surgical glue. The mice were given an antibiotic (ampicillin, 125 mg/kg, i.m.) and an analgesic (ketoprofen, 4 mg / kg. i.p.) followed by atipamezole (Antisedan, 2mg/kg s.c., an agent that reverses the sedative effect of dexmedetomidine). The mice were placed for 2 hours in a humidified 37 °C environment to recover and then were returned to regular cages. The mice received a second round of antibiotic and analgesic treatment the next day before being returned to the vivarium. Mice survived 4-6 weeks before perfusion.

Perfusions

The mice were deeply anesthetized with pentobarbital (60 mg/kg i.p.), and perfused through the heart with 10 ml of phosphate buffered saline (pH 7.4) followed by 75 ml of 4% phosphate-buffered (0.1 M; pH 7.4) paraformaldehyde (Electron Microscopy Sciences, Fort Washington, PA). Series of coronal sections (30 μm) from the brain were cut using a vibrating microtome and stored in cryoprotectant solution at −20° C (20% glycerol plus 30% ethylene glycol in 50 mM phosphate buffer, pH 7.4) awaiting histological processing.

Histology

Immunocytochemical detection of ChAT, GFP, TH, mCherry—Sections were rinsed in 0.1M Tris buffered saline pH 7.4 (TBS), then blocked for non-specific immunoreactivity by 30 minute incubation with 10% horse serum and 0.3% triton in Tris-buffered saline. ChAT was identified using a goat antibody (1:100, Millipore) followed by either a Cy3-tagged donkey anti-goat IgG (1:200, Jackson) or an Alexa 488-tagged donkey anti-goat IgG (1:200, Molecular Probes, Invitrogen). GFP was identified with a rabbit antibody (1:10,000, Stratagene) followed by an Alexa 488-tagged donkey anti-rabbit IgG (1:200, Molecular Probes, Invitrogen). In some cases, GFP was processed with the same primary antibody but with a biotinylated donkey anti-rabbit IgG (1:500, Jackson) followed by the ABC kit (Vector) and subsequent colorization with 3-3′ di-aminobenzidine (DAB) using the DAB peroxidase substrate kit according to manufacturer's instructions (Vector). TH was identified with a sheep antibody (1:2000, Millipore) followed by an Alexa 488-tagged donkey anti-sheep IgG (1:200, Jackson). In cases with double immuno-labeling for ChAT and TH, the sections were first reacted for TH using the same sheep TH antibody, then incubated with a biotinylated donkey anti-sheep IgG (1:1000, Jackson) followed by the ABC kit (Vector) and subsequent colorization with a solution of 0.1 % nickel chloride and 0.1 % DAB (DAB peroxidase substrate kit according to manufacturer's instructions, Vector) yielding a black reaction product and then reacted for ChAT using the goat anti-ChAT antibody and subsequent colorization with DAB (as described above) yielding a brown reaction product. ChR2-mCherry was identified with a rabbit antibody to DsRed (1:500, ClonTech) followed by Cy3-tagged donkey anti-rabbit IgG (1:200, Jackson).

Antibody characterizations

Goat anti-ChAT polyclonal antibody: (Millipore #AB144P) was raised against the human placental enzyme. Western blots of mouse brain lysates showed a single band corresponding to the expected 70/74 kDa molecular weight (manufacturer's information). The pattern of

labeling produced in the current study is seen in cell soma, dendrites and axons and was restricted to previously described cholinergic cell groups (Ruggiero et al., 1990; Ichikawa et al., 1997).

Rabbit anti-hrGFP polyclonal antiserum: (Stratagene #240142) was raised against the full length humanized form of recombinant *R. reniformis* GFP. Western blot analysis against transfected HEK 293 cells produced a single band of 32.5 kDa corresponding to hrGFP (manufacturer's information). Gautron and colleagues (2010) used this antiserum to detect AAVmediated expression of hrGFP using an identical viral vector in the mouse brain. The labeling we observed using this antibody was present throughout the cytoplasm in both cell bodies and projections including fibers and boutons. No immunoreactivity was seen in brain sections from uninjected ChAT-Cre mice (data not shown).

Sheep anti-TH polyclonal antibody: (Millipore #AB1542) was raised against native TH from rat pheochromocytoma. Western blot analysis using a 1:1000 dilution of antibody on 10 of mouse brain tissue lysates revealed a single band at the predicted molecular weight of ~ 60 kDa. Positive controls included caudate striatum and adrenal gland. No staining was observed in liver (manufacturer's information). The pattern of labeling we observed in the brainstem was identical to that seen in mice previously by others (Chen et al. 2010).

Rabbit anti-DsRed antibody: (Clontech #632496) was raised against DsRed-express, a variant of *Discosoma* sp. red fluorescent protein that recognizes both N- and C-terminal fusion proteins containing DsRed variants (including mCherry). Western blot analysis using lysates from HEK 293 cells stably expressing DsRed-express revealed a single band of 30-38 kDa. No band in this molecular weight range was seen in Westerns from lysates of untransfected cells or from cells expressing AcGFP1 (manufacturer's information). No labeling was seen in brains from mice without virus injections.

Mapping—A one in three series of 30 μm coronal sections through the brain were examined for each experiment under bright field and epifluorescence using a Zeiss AxioImager Z.1 microscope (Carl Zeiss Microimaging, Thornwood, NY). Coronal spinal cord sections were randomly sampled from all levels within cervical, thoracic and lumbar cord. At least 20 spinal cord sections from within each general spinal cord division were sampled per animal. Neurons immunoreactive for ChAT, TH, GFP, mCherry or natural FG fluorescence were plotted with the Neurolucida software (Micro Brightfield, Colchester, VT) utilizing a Ludl motor driven microscope stage and the Zeiss MRC camera, after methods previously described (Stornetta et al. 2004). Filter settings for the Cy3, Alexa 488 and FG fluorophores were as follows: FG, excitation of 365 nm and emission filter of 420 nm; Alexa 488, excitation of 500 nm, emission of 535 nm; Cy3, excitation of 545, emission of 605 nm. Only cell profiles that included a nucleus were counted and/or mapped. Cell measurements were made by tracing the outline of the cell body and using the Neurolucida software contour measurements to determine cell area. The Neurolucida files were exported into the Canvas drawing software (Version 10, ACD Systems, Inc.) for text labeling and final presentation. The neuroanatomical nomenclature is after Paxinos and Franklin (2004). Photographs were taken with a Zeiss MRC camera (resolution 1388 × 1040 pixels) and the resulting TIFF files were imported into the Canvas software. Output levels were adjusted to include all information-containing pixels. Balance and contrast was adjusted to reflect true rendering as much as possible. No other "photo-retouching" was done. Figures were assembled and labeled within the Canvas software.

Results

Location and size of the mRVLM-ChAT neurons in mice

The RVLM is usually defined as a roughly triangular wedge of the medulla oblongata defined by the nucleus ambiguous dorsally, the lateral edge of the pyramidal tract or inferior olive medially and, laterally, by the medial edge of the trigeminal tract (Fig.1). This region corresponds closely to the retrofacial aspect of nucleus paragigantocellularis according to Andrezik et al. (1981). We refer to the medial corner of this region, located lateral to the pyramidal tract or inferior olive, as the mRVLM. As illustrated in Fig. 1, this region of the mouse brain contains a cluster of ChAT-immunoreactive (ir) neurons that are relatively well segregated from the cholinergic neurons that populate the nucleus ambiguus, the facial motor nucleus and the ventromedial medulla (VMM in Fig.1). The dorsal half of the medulla oblongata contains additional cholinergic cell groups that are not represented in Fig. 1. The cluster of mRVLM ChAT-ir neurons appears at a coronal level slightly anterior to the obex (7.6 mm caudal to bregma in Fig. 1) and continues rostrally to the caudal end of the facial motor nucleus (6.4 mm caudal to bregma in Fig.1). The boundary between the mRVLM ChAT-ir neurons and the cholinergic neurons that reside in the ventromedial medulla (VMM) is less obvious at rostral levels (Fig.1) but the small size of the mRVLM ChAT-ir neurons is a helpful distinguishing feature. Indeed, the somata of the mRVLM ChAT-ir neurons have an average cross section of only 91 ± 3 μm^2 in the transverse plane which is considerably smaller ($p<0.0001$ by ANOVA) than neighboring clusters of lower brainstem cholinergic neurons (cells sizes determined from 20-40 neurons mapped per area from 3 different mice). The other ChAT-ir neurons selected for comparison were facial motor neurons (499 ± 11 μm^2), nucleus ambiguus motor neurons (308 ± 13 μm^2) and neurons located within the rostral VMM (364 ± 18 μm^2). The latter were located dorsomedial to the mRVLM (Fig.1: VMM, transverse levels 6.4 to 6.8 mm caudal to bregma).

mRVLM-ChAT neurons are neither parasympathetic preganglionic neurons nor cranial motor neurons

The ventrolateral medulla contains motor neurons that regulate the esophagus or airway muscles and parasympathetic preganglionic neurons that target the heart and lungs (Bieger and Hopkins, 1987; Standish et al., 1995). The next experiments were designed to ascertain that the mRVLM-ChAT neurons were neither motor neurons nor parasympathetic preganglionic neurons.

After i.p. injection, Fluorogold (FG) was detected in cells in the expected regions namely the area postrema, all lower brainstem motor neurons (facial, hypoglossal, nucleus ambiguus) and in readily identified (dorsal motor nucleus of the vagus, salivary nuclei) or putative parasympathetic preganglionic neurons (ventrolateral medulla; for examples see Fig. 2). The mRVLM-ChAT neurons did not contain FG (zero FG-containing neurons detected in 10 sections spanning bregma levels 7.64 -6.36 mm from 3 mice, for examples see Fig. 2). Therefore, the mRVLM-ChAT neurons lie within the blood brain barrier and do not project outside the brain. The location of ChAT-ir neurons that were FG positive and those lacking this marker (motor neurons and putative parasympathetic neurons) is shown for a representative mouse in Fig. 1. Note that within the ventrolateral medulla, the mRVLM-ChAT neurons form a distinctive cluster of cells without projections outside the brain.

mRVLM-ChAT neurons express GFP or mCherry selectively after injection of floxed AAV2 into ChAT-Cre mice

GFP immunoreactivity was detected exclusively within ChAT-ir neurons in all 4 cases in which AAV2-floxed-GFP was targeted to the region that contains these neurons (Fig. 3a,b).

Identical results were obtained following injection of AAV2-floxed-ChR2-mCherry into the same region (4 mice). No differences in transduction or projection patterns were discernible between sexes, although only one female was represented in either virus group (GFP2 and CR1 were females, the rest were males). Within the terminal fields of the GFP-projecting neurons, axonal varicosities or boutons were also ChAT-ir (Fig. 3c,d). Fig. 4 illustrates a case in which injections of AAV2-floxed-GFP into mRVLM resulted in almost all mRVLM-ChAT neurons located in the rostral two thirds of this cell group (89% of the ChAT-ir neurons confined to the mRVLM or 76% of ChAT-ir neurons including the entire RVLM) expressing GFP. Typically, a smaller proportion of the mRVLM-ChAT neurons were labeled. The location of the transduced ChAT-ir neurons (i.e. GFP-ir) is shown in Fig. 5 for the 4 mice injected with floxed-GFP-AAV2. Fig. 6 illustrates the location of the mCherry-transduced ChAT-ir neurons for the 4 mice that received injections of AAV2-floxed-ChR2-mCherry. Although the mCherry vector cases had more neurons transduced overall than the GFP vector cases (mean number transduced cells counted in a one in three series of coronal sections in mCherry vector cases 42 ± 8 vs. 27 ± 7 neurons in the GFP vector cases), the “extra” neurons were predominantly in and dorsal to the area of the facial motor nucleus of two of the mCherry vector cases. When examining specifically the mRVLM neurons, the mCherry vector resulted in about the same number of transduced mRVLM neurons (27 ± 2 neurons counted in the mCherry cases). The distribution of transduced neurons was slightly shifted to the rostral level in the mCherry vector cases (Fig. 6). There were no discernible differences in projection patterns related to any differences in the rostro-caudal distribution or numbers of transduced neurons, however, the amount of labeling was greater in the terminal fields of the cases with more neurons were labeled.

Axonal projections of the mRVLM-ChAT neurons in the ChAT-Cre mouse

The transgene product (GFP or mCherry) was detected throughout the mRVLM-ChAT neurons, including soma, dendrites, axons and terminals, cytoplasm and membranes. Examples of terminal fields labeled with GFP are shown in Fig. 3 and Figs. 7-9; examples of mCherry labeled terminal fields are shown in Fig. 10. Areas were deemed to receive projections if labeled fibers had visible terminal boutons or en-passant varicosities. The labeled axons crossed the midline around 6.5 mm caudal to bregma (levels according to the atlas of Paxinos and Franklin (2004)) and /or proceeded rostrally on the ipsilateral side (Fig. 8). In the spinal cord, projections with a contralateral predominance were seen only in layer III of the dorsal horn at all levels examined (cervical, thoracic and lumbar, Fig.10). Dense terminal fields were observed in both gracile and cuneate nuclei with a slight contralateral predominance (Fig. 7). Projections with a contralateral predominance were also noted to the spinal trigeminal nucleus, particularly to the caudal and dorsomedial parts but mostly avoiding the interpolar region. Sparse projections were noted in the nucleus of the solitary tract, mostly lateral and ventral to the tract. Thin fibers with multiple varicosities were observed in the immediate vicinity of the labeled mRVLM-ChAT somata, suggesting that these neurons have local, possibly recurrent, collaterals within the mRVLM (Fig. 8b_1,b_2). Labeled terminals were also found in the vicinity of mRVLM-ChAT neurons located on the side contralateral to the injection of the viral vector (Fig.8c). The dorsal aspects of the superior olivary nucleus received heavy projections with a contralateral predominance in all cases (Fig. 9). The dorsal cochlear nucleus was also a target in all cases, although no contralateral predominance was noted (Fig. 9). The cerebellum received a very sparse innervation that was detected only in some cases. Terminal fields were observed in most cases in the periaqueductal gray, with a slight contralateral predominance (Fig. 9). About half the cases had some innervation of the inferior colliculus (Fig. 9). There was also sparse innervation of the dorsolateral aspect of the parabrachial nucleus in some cases. Fibers with en-passant boutons were observed consistently within the lateral lemniscus in all cases. The more rostral midbrain was preserved in only one case. In this mouse, sparse terminals were

observed in the medial geniculate nucleus. The diencephalon and forebrain were examined in all cases. These regions contained no detectable projections.

Projections of RVLM catecholaminergic neurons traced after injections of floxed-ChR2-mCherry AAV2 into DBH-Cre mice

The RVLM of the mouse contains TH-ir neurons that are presumably homologous to the C1 adrenergic group of other species (Hokfelt et al. 1974; Ross et al. 1983; Card et al., 2006; Chen et al., 2010). The location of these catecholaminergic neurons overlaps considerably with that of the mRVLM-ChAT neurons as is readily apparent when coronal sections of the mouse brain are reacted for simultaneous detection of ChAT and TH (Fig. 11a).

Four to six weeks after injection AAV2-floxed-ChR2-mCherry into the RVLM of DBH-Cre mice, mCherry-ir somata were confined to the RVLM and were essentially all TH-ir. A typical injection site is shown in Fig. 11b. The rostrocaudal distribution of the mCherry-labeled somata is shown in Fig. 11c from a representative case in which 67% of the TH-ir neurons in the RVLM were transduced. In every case the mCherry-labeled neurons were confined to the ipsilateral RVLM, i.e. the other groups of catecholaminergic neurons of the medulla oblongata or pons (nucleus solitary tract, dorsomedial medulla, locus coeruleus and A5) were not transduced.

In these mice, the mCherry-positive axonal processes were found in all the regions previously identified as receiving projections of C1 adrenergic neurons in the rat (Card et al., 2006). Fig. 12 illustrates some of the targets of the TH-ir neurons of the mouse RVLM and the Table compares and contrasts the projections of these neurons to those of the adjacent mRVLM-ChAT neurons. As the next few examples will highlight, the projections of the two different cell types were essentially non-overlapping. In the dorsal medulla, the TH neurons massively targeted the dorsal vagal complex (nucleus of the solitary tract, area postrema and dorsal motor nucleus of the vagus) and avoided the dorsal column nuclei (Fig. 12a,a_1), in striking contrast to the mRVLM-ChAT cells. The spinal projections of the TH neurons targeted exclusively the intermediolateral cell column and the region surrounding the central canal (Fig. 12b,b_1) whereas the mRVLM-ChAT neurons innervated lamina III of the dorsal horn exclusively (Fig.10). The TH neurons had no projections to the trigeminal complex, the cochlear nucleus or the superior olive, contrary to the mRVLM-ChAT neurons. The TH neurons heavily targeted the locus coeruleus (LC) and the dorsolateral parabrachial complex (dPBN) which received no (LC) or very sparse (dPBN) projections from the mRVLM-ChAT neurons (data not shown).

Discussion

The present study suggests that the cholinergic neurons of the medial RVLM regulate the transmission of somatosensory and auditory stimuli rather than cardiorespiratory and other autonomic functions. From a functional standpoint, the mRVLM cholinergic neurons should therefore be considered as a lateral extension the ventromedial medulla rather than a component of the ventrolateral medulla.

Technical considerations

In order to correctly trace the projections of chemically defined CNS neurons using a Cre-dependent viral vector, it is essential to ascertain that the targeted neurons are selectively transduced (Fenno et al. 2011). In the present case, such selectivity was established by showing that the same Cre-dependent AAV2 was capable of transducing two separate neuronal phenotypes in different Cre-driver mice (ChAT-ir neurons in the ChAT-Cre mouse and catecholaminergic neurons in the DBH-Cre mouse).

The selectivity of a Cre-dependent vector depends on the accuracy of Cre expression by the transgenic mice of interest, in their adult state. The first potential problem is a hypothetical ectopic expression of Cre recombinase within the region of interest. There was no ectopic expression in the present cases since every mCherry-positive neuron contained ChAT in the ChAT-Cre mice and virtually all the mCherry-positive neurons contained TH immunoreactivity in the DBH-Cre mice. The second issue is whether Cre is expressed by all or only by a subset of the targeted neuronal groups. We could not answer this question definitively in the present experiments because the AAV2 typically transduced only a fraction of the mRVLM-ChAT neurons. Nonetheless, based on the case illustrated in Fig. 4 in which the majority of the mRVLM-ChAT neurons were transduced, it seems likely that most if not all of the mRVLM-ChAT neurons do express Cre in the ChAT-Cre mouse line that we used and that these neurons were transduced at random by the vector in different mice. However, we cannot entirely exclude the possibility that the projections traced in the present study originated from a subset of these neurons. A similar caveat is in order with regard to the projections of the RVLM catecholaminergic neurons that were traced in the DBH-Cre mice.

Finally, given the very small size of the mouse brain, anterograde tract-tracing using a Cre-dependent virus requires a vector that does not propagate retrogradely and remains confined to a small brain region following injection. These attributes are needed to avoid ambiguity as to the cells of origin of the axonal projections. We confirm that the serotype 2 version of the AAV has the required properties (Chamberlin et al. 1998). For example, the pontine cholinergic neurons that abundantly innervate the RVLM (Yasui et al. 1990) did not express the transgene in any of the ChAT-Cre mice. Similarly, no evidence of retrograde labeling was seen in the experiments in which AAV2-floxed-ChR2-mCherry had been administered to DBH-Cre mice.

Projections of the C1 neurons in the mouse

The projections of the C1 neurons have been the subject of numerous studies since the recognition of their potential importance in blood pressure control, c.f. (Hökfelt et al., 1974; Coote and Macleod 1974; Chalmers et al. 1981; Ross et al. 1981; Sawchenko and Swanson 1982; Sawchenko et al. 1985; Routledge and Marsden 1987; Tucker et al. 1987; Cunningham, Jr. and Sawchenko 1988; Reis et al. 1988; Wesselingh et al. 1989; Haselton and Guyenet 1990; Maisky and Doroshenko 1991; Jansen et al. 1995). These studies provided a piecemeal and incomplete picture of the projections of the C1 neurons. A more comprehensive description of these projections has appeared in a recent study in which the authors labeled these neurons selectively using a lentiviral vector that expresses GFP under the control of the artificial catecholamine neuron-preferring PRSx8 promoter (Card et al., 2006). The present results suggest that the projection pattern of the C1 neurons is similar in rats and mice.

Prior evidence for mRVLM-ChAT neurons and species homologies

A cluster of ChAT-ir neurons has been identified in the mRVLM of all species investigated including mouse (present study), rat (Ruggiero et al., 1990), cat (Holmes et al. 1994) and guinea pig (Motts et al. 2008) although a few reports have not specifically illustrated this cell group in their survey of CNS ChAT-ir neurons, e.g. (Armstrong et al. 1983; Ichikawa et al., 1997). The relatively low level of cholinergic markers present in the cell bodies of the mRVLM-ChAT neurons is probably due to their small size and explains why these neurons were overlooked in a few studies. VAChT is required for the vesicular packaging and exocytotic release of acetylcholine, therefore this protein is considered as a diagnostic marker of cholinergic neurons (Chaudhry et al., 2008). The Allen Mouse Brain Atlas (Allen Mouse Brain Atlas [Internet], 2009) shows neurons located in the mRVLM of the mouse

that contain VAChT transcripts and we found that the cell bodies of the mRVLM-ChAT neurons of rats contain readily detectable levels of VAChT mRNA (unpublished data by Dr. R. Stornetta). In the aggregate, the evidence indicates that the mRVLM-ChAT neurons are bona fide cholinergic neurons. The opposite view (Padley et al. 2007) was based on these authors' failure to identify VAChT immunoreactivity in the soma of these neurons in rats. Given that the cognate mRNA is present in these neurons (unpublished data by Dr. R. Stornetta), this negative result can be most readily explained by the fact that VAChT, like the other vesicular transporters that are exported to the terminals, is present at very low levels in cell bodies and therefore is difficult to identify by immunohistochemistry in this cell compartment.

The mRVLM-ChAT neurons may also produce additional transmitters. In the rat, a small subset of ChAT-ir neurons located in this region also contain GAD67 mRNA and therefore may be GABAergic (Schreihofer and Guyenet 2003). The mRVLM-ChAT neurons may also release nitric oxide because the mRVLM contains neurons that express NADPH diaphorase activity in rat (Iadecola et al. 1993) and mRNA transcripts for neuronal nitric oxide synthase in mice (Allen Mouse Brain Atlas [Internet], 2009). In further support of this speculation, the gracile nucleus which, as shown here, is a major target of the mRVLM-ChAT neurons, contains a dense network of fibers that are immunoreactive for nitric oxide synthase (Dun et al. 1994).

Projections of the mRVLM-ChAT neurons

The projections of the RVLM have been extensively studied (Swanson and Hartman 1975; Loewy et al. 1981; Ruggiero et al. 1989; Guyenet and Stornetta 2004) but no one has attempted to pin down the specific projections of the cholinergic cells located within this region. Jones (1990) described cholinergic neurons in the lateral paragigantocellular area of the rat which were retrogradely labeled after large injections of tracer into the pontine tegmentum and concluded that these cholinergic neurons "may not only be visceral motor neurons... but also be centrally projecting neurons". The Fluorogold experiment described herein indicates quite clearly that the mRVLM-ChAT neurons are neither motor neurons nor parasympathetic preganglionic and that these cells do innervate the pons. Jones also raised the possibility that the cholinergic neurons of the lateral paragigantocellular area of the cat have axonal collaterals in the region of their cell bodies. This feature was identifiable in the case of the mRVLM-ChAT neurons of the mouse which suggest that the medullary cholinergic neurons described by Jones could be homologous to the rodent mRVLM-ChAT neurons.

However, we suggest the study most pertinent to the present one is that of Kamiya et al. (1988) despite the fact that ChAT is not mentioned in their study. These authors focused on a cluster of small neurons located in the RVLM of cats next to the pyramidal tract, which they could identify in this species on purely cytoarchitectonic grounds (1988). This neuronal cell group, termed the ventrolateral medullary nucleus (VLMN), was shown to innervate the dorsal column nuclei and the cochlear nuclei which, as noted here, are prominent targets of the murine mRVLM-ChAT neurons. Thus, the VLMN of Kamiya et al. (1988) likely consists of, or includes, cholinergic neurons that are homologous to the mRVLM-ChAT neurons of mice. WGA-HRP, used by these authors as an anterograde tracer, is also avidly transported in a retrograde fashion from the injection site and retrogradely labeled neurons could have been the source of some of the labeled terminal fields causing some potential ambiguity regarding their origin. However, we fully confirm the heavy bilateral projections, commonly with modest contralateral predominance, of the mRVLM neurons to the dorsal column nuclei, the central gray, the inferior colliculus and the cochlear nuclei described by Kamiya et al. (1988). We also found substantial projections to brain regions that were not mentioned by Kamiya et al. (1988) such as the superior olivary complex, the spinal

trigeminal nucleus and the dorsal horn of the spinal cord. These differences may be species related but they could also be explained by the very small number of cats studied by Kamiya et al. (1988) or by the possible existence of subsets of mRVLM-ChAT neurons with distinct projections.

mRVLM-ChAT neurons and sensory afferent information processing

The lack of innervation of the locus coeruleus, the hypothalamus and the raphe by mRVLM-ChAT neurons suggests that these neurons, contrary to the neighboring C1 neurons, are not directly involved in breathing, autonomic regulations or arousal (Aston-Jones et al. 2001; Lu et al. 2006; Jensen et al. 2008; Fuller et al. 2011). Also, mRVLM-ChAT neurons do not target spinal nor pontomedullary regions that harbor motor neuronal pools (hypoglossal, facial, trigeminal, ambigual) and therefore these cholinergic neurons are presumably not, or least not directly, involved in lung, visceral and somatic motor control. In this regard, the projections of the mRVLM-ChAT neurons are also very different from those of the nearby serotonergic neurons of the raphe obscurus and pallidus which heavily target lower brainstem and spinal motor neurons, the RVLM, the dorsal medulla, the deep laminae of the spinal cord and the intermediolateral cell column consistent with their postulated role in the state-dependent regulation of thermogenesis, cardiorespiratory function and somatic motor outflows (Allen and Cechetto 1994; Veasey et al. 1997; Ptak et al. 2009; Depuy et al. 2011). The projections of the mRVLM-ChAT neurons also set them clearly apart from the network of neurons that control breathing movements. The latter network interconnects a well-defined set of structures that is almost totally eschewed by mRVLM-ChAT neurons (Kölliker-Fuse, inter-trigeminal region and lateral parabrachial nuclei in the pons, caudal nucleus tractus solitarius, retrotrapezoid nucleus and all segments of the ventral respiratory column) (Alheid and McCrimmon, 2008; Smith et al., 2009; Tan et al. 2010; Bochorishvili et al. 2011)

The inferior olive projects massively to the cerebellum (climbing fibers). As mentioned above, we found no evidence of GFP or mCherry expression by inferior olivary neurons in the five cases in which labeled axons and terminals were present in the cerebellum. We therefore assume that the sparse cerebellar innervation that we detected after virus injection into the mRVLM originated from ChAT-ir neurons, not from inferior olivary neurons. The cerebellum contains ChAT-ir “beaded fibers” (Jaarsma et al. 1997) and the lateral paragigantocellular nucleus, a region that includes the area of distribution of the mRVLM-ChAT neurons, was among the postulated sources of this cholinergic innervation (Andrezik et al. 1981; Jaarsma et al., 1997). The significance of the cerebellar projection is difficult to predict from the current results because it was extremely sparse and was not consistently observed in the same cerebellar region (e.g. cerebellar cortex, various deep cerebellar nuclei). One possibility is that the rare cerebellar projections that we observed originated from a few cholinergic neurons located at the outer margins of the mRVLM and which were inconsistently transduced in our experiments.

The core set of structures targeted most heavily and consistently by the mRVLM-ChAT neurons suggests that the main function of these neurons is to modulate the processing of selected general and special sensory information, especially hearing. The heavy projections to the cuneate and gracile nucleus suggest that the mRVLM-ChAT neurons regulate sensations of fine touch and proprioception rather than nociception or temperature (Whitsel et al. 1972). Their projections to lamina III of the spinal cord but not to lamina I and II also reinforces this interpretation (Todd 2010). Fernandez de Sevilla et al. (2006) showed that muscarinic cholinergic agonists amplify the response of gracile neurons to sensory afferent stimulation. mRVLM-ChAT neurons therefore presumably facilitate transmission through the dorsal column nuclei. Fernandez de Sevilla et al. (2006) suggested, however, that the main cholinergic input to the gracile nucleus originates from the pontine reticular formation

(PRN) rather than from the mRVLM and they supported this claim by providing evidence that electrical stimulation of the PRN facilitates transmission through the gracilis nucleus. However, this facilitation could also conceivably have been produced, in part at least, via activation of the mRVLM-ChAT neurons since the axons of these neurons decussate within and innervate the pontine reticular formation.

The innervation of the superior olivary complex, cochlear nucleus, lateral lemniscus nuclei, inferior colliculus and medial geniculate nuclei suggest that the mRVLM-ChAT neurons modulate auditory or vestibular afferent inputs. Projections from the ventral medulla to the cochlear nucleus have been described previously (Kamiya et al., 1988; Dehmel et al. 2008). Our results indicate that they originate, at least in part, from the mRVLM-ChAT neurons.

mRVLM-ChAT neurons and cardiorespiratory regulation

The RVLM contains several categories of well-characterized neurons that regulate breathing and the circulation (Guyenet, 2006; Feldman and Del Negro 2006; Coote 2007; Smith et al., 2009; Tan et al., 2010; Bochorishvili et al., 2011). These neurons interconnect the so-called “respiratory column” (a region with major overlap with the RVLM), the dorsal medulla oblongata (e.g. nucleus of the solitary tract), the intermediate reticular nucleus, the dorsolateral pons (lateral parabrachial region and Kölliker-Fuse nucleus) plus various pools of brainstem and spinal motor neurons (Ellenberger and Feldman 1990; Stocker et al. 1997; Cream et al. 2002; Weston et al. 2004; Rosin et al. 2006; Alheid and McCrimmon, 2008; Abbott et al. 2009). The C1 adrenergic neurons, which are activated by somatic and visceral stresses (e.g. pain or hypoxia) and better known for their role in blood pressure control, target many of the same structures plus the raphe, the retrotrapezoid nucleus, the intermediolateral cell column, various groups of noradrenergic neurons including the locus coeruleus and several midbrain and hypothalamic regions associated with autonomic or endocrine responses to stress (e.g. CRF-producing paraventricular neurons) (Ericsson et al. 1994; Guyenet, 2006; Card et al., 2006). The mRVLM-ChAT neurons have essentially no projection to these brain areas. They seem to have a few axonal collaterals within the ventrolateral medulla on both sides but these collaterals remain in close proximity to their cell bodies. Accordingly, the mRVLM-ChAT neurons are unlikely to directly control the activity of the nearby breathing network. In addition, the mRVLM-ChAT neurons innervate neither the medullary raphe nor the retrotrapezoid nucleus nor the locus coeruleus, therefore they probably do not contribute directly to central respiratory chemoreception (Guyenet et al. 2008; Nattie and Li 2009; Guyenet et al. 2010). Finally, the projections of the mRVLM-ChAT neurons to the regions innervated by the C1 cells are at best exceedingly light suggesting that these cholinergic neurons do not directly regulate the cardiovascular system or the neuroendocrine responses to stress. Projections of the mRVLM-ChAT neurons to the raphe magnus region and to the raphe pallidus are also essentially nonexistent suggesting that these cholinergic neurons contribute little to thermoregulation (Morrison et al. 2008).

Yet, the ventrolateral medulla receives a dense cholinergic innervation and the cardiorespiratory circuitry is strongly activated by acetylcholine (Punnen et al., 1986; Giuliano et al., 1989; Huangfu et al., 1997; Shao et al., 2008). One known source of this cholinergic innervation is the pedunculopontine nucleus which presumably regulates the cardiorespiratory outflows in a state-dependent manner or in relation to physical exercise (Yasui et al., 1990; Padley et al., 2007). The sparse projections of the mRVLM-ChAT neurons to the adjacent ventrolateral medulla indicate that these neurons make at best a modest contribution to the cholinergic regulation of the adjacent cardiorespiratory network. The projections of the mRVLM-ChAT neurons to the ipsi and contralateral mRVLM suggest the mRVLM-ChAT neurons themselves may have recurrent interactions.

Conclusions

The RVLM plays a key role in breathing, circulatory control, stress responses, the regulation of cortical activity and the control of cerebral blood flow (Ennis et al., 1992; Golanov et al., 2000; Sawchenko et al., 2000; Guyenet, 2006; Li et al., 2009; Smith et al., 2009; Feldman et al., 2009). Its medial aspect, the mRVLM, contains small cholinergic neurons which, given their projections, are unlikely to be regulating any of the above functions. Instead, these cholinergic neurons appear to selectively control incoming sensory discriminative or proprioceptive information and also appear to regulate hearing or at least behaviors facilitated by auditory stimuli. The direction of the bias is uncertain but is likely to be positive given the effect of acetylcholine on the gracile nucleus (Fernandez de Sevilla et al. (2006)). The mRVLM-ChAT cells are located only slightly caudal and lateral to the region of the medulla oblongata that regulates the transmission of nociceptive inputs (for reviews: (Fields et al. 1991; Basbaum et al. 2009)). Given their apparent specialization in sensory control and lack of connection with regions implicated in cardiorespiratory and autonomic regulations, the mRVLM-ChAT cells should perhaps be classified as a lateral extension of the ventromedial medulla (VMM) rather than as a part of the ventrolateral medulla.

Acknowledgments

This work was supported by the following grants from the National Institutes of Health (HL74011 & HL 28785 to PGG).

List of abbreviations

7	facial motor nucleus
10	dorsal motor nucleus of the vagus
12	hypoglossal motor nucleus
AAV	adeno-associated viral vector
Amb	ambiguus nucleus
AP	area postrema
CC	central canal
ChAT	choline acetyl transferase
CHT1	choline transporter
Cu	cuneate nucleus
cu	cuneate fasciculus
DBH	dopamine beta hydroxylase
DC	dorsal cochlear nucleus
dlPBN	dorsal lateral parabrachial complex
FG	Fluorogold
GFP	green fluorescent protein
Gr	gracile nucleus
IC	inferior colliculus
ION	inferior olivary nucleus

LL	lateral lemniscus
LRt	lateral reticular nucleus
ml	medial lemniscus
mRVLM	medial part of the RVLM
PAG	periaqueductal gray
PRN	pontine reticular formation
py	pyramidal tract
pyx	pyramidal decussation
RMg	raphe magnus
RVLM	rostral ventrolateral medulla
scp	superior cerebellar peduncle
Sol	nucleus of the solitary tract
SON	superior olivary nucleus
Sp5C	spinal trigeminal nucleus caudal
Sp5DM	spinal trigeminal nucleus, dorsomedial
Sp5I	spinal trigeminal nucleus, interpolar
sp5	spinal trigeminal tract st, solitary tract
TH	tyrosine hydroxylase
Tz	nucleus of the trapezoid body
VAChT	vesicular acetylcholine transporter
VLMN	ventrolateral medullary nucleus (cat)
VMM	ventromedial medulla

LITERATURE CITED

Allen Mouse Brain Atlas [Internet]. Allen Institute for Brain Science; Seattle, WA: 2009. Available from: http://mouse.brain-map.org

Abbott SB, Stornetta RL, Fortuna MG, Depuy SD, West GH, Harris TE, Guyenet PG. Photostimulation of retrotrapezoid nucleus Phox2b-expressing neurons in vivo produces long-lasting activation of breathing in rats. J Neurosci. 2009; 29:5806–5819. [PubMed: 19420248]

Alheid GF, McCrimmon DR. The chemical neuroanatomy of breathing. Respir Physiol Neurobiol. 2008; 164:3–11. [PubMed: 18706532]

Allen GV, Cechetto DF. Serotoninergic and nonserotoninergic neurons in the medullary raphe system have axon collateral projections to autonomic and somatic cell groups in the medulla and spinal cord. J Comp Neurol. 1994; 350:357–366. [PubMed: 7533797]

Andrezik JA, Chan-Palay V, Palay SL. The nucleus paragigantocellularis lateralis in the rat: Conformation and cytology. Anat Embryol. 1981; 161:355–371. [PubMed: 7247034]

Armstrong DM, Saper CB, Levey AI, Wainer BH, Terry RD. Distribution of cholinergic neurons in rat brain: demonstrated by the immunocytochemical localization of choline acetyltransferase. J Comp Neurol. 1983; 216:53–68. [PubMed: 6345598]

Aston-Jones G, Chen S, Zhu Y, Oshinsky ML. A neural circuit for circadian regulation of arousal. Nat Neurosci. 2001; 4:732–738. [PubMed: 11426230]

Basbaum AI, Bautista DM, Scherrer G, Julius D. Cellular and molecular mechanisms of pain. Cell. 2009; 139:267–284. [PubMed: 19837031]

Bieger D, Hopkins DA. Viscerotopic representation of the upper alimentary tract in the medulla oblongata in the rat: the nucleus ambiguus. J Comp Neurol. 1987; 262:546–562. [PubMed: 3667964]

Bochorishvili G, Stornetta RL, Coates MB, Guyenet PG. Pre-Botzinger complex receives glutamatergic innervation from galaninergic and other retrotrapezoid nucleus neurons. J Comp Neurol. 2011; 520:1047–1061. [PubMed: 21935944]

Card JP, Sved JC, Craig B, Raizada M, Vazquez J, Sved AF. Efferent projections of rat rostroventrolateral medulla C1 catecholamine neurons: Implications for the central control of cardiovascular regulation. J Comp Neurol. 2006; 499:840–859. [PubMed: 17048222]

Cardin JA, Carlen M, Meletis K, Knoblich U, Zhang F, Deisseroth K, Tsai LH, Moore CI. Driving fast-spiking cells induces gamma rhythm and controls sensory responses. Nature. 2009; 459:663–667. [PubMed: 19396156]

Chalmers JP, Blessing WW, West MJ, Howe PR, Costa M, Furness JB. Importance of new catecholamine pathways in control of blood pressure. Clinical & Experimental Hypertension. 1981; 3:393–416. [PubMed: 6265166]

Chamberlin NL, Du B, de LS, Saper CB. Recombinant adeno-associated virus vector: use for transgene expression and anterograde tract tracing in the CNS. Brain Res. 1998; 793:169–175. [PubMed: 9630611]

Chaudhry FA, Boulland JL, Jenstad M, Bredahl MK, Edwards RH. Pharmacology of neurotransmitter transport into secretory vesicles. Handb Exp Pharmacol. 2008; 184:77–106. [PubMed: 18064412]

Chen D, Bassi JK, Walther T, Thomas WG, Allen AM. Expression of angiotensin type 1A receptors in C1 neurons restores the sympathoexcitation to angiotensin in the rostral ventrolateral medulla of angiotensin type 1A knockout mice. Hypertension. 2010; 56:143–150. [PubMed: 20458002]

Coote JH. Landmarks in understanding the central nervous control of the cardiovascular system. Exp Physiol. 2007; 92:3–18. [PubMed: 17030558]

Coote JH, Macleod VH. The influence of bulbospinal monoaminergic pathways on sympathetic nerve activity. J Physiol. 1974; 241:453–475. [PubMed: 4548438]

Cream C, Li A, Nattie E. The retrotrapezoid nucleus (RTN): local cytoarchitecture and afferent connections. Respir Physiol Neurobiol. 2002; 130:121–137. [PubMed: 12380003]

Cunningham ET Jr. Sawchenko PE. Anatomical specificity of noradrenergic inputs to the paraventricular and supraoptic nuclei of the rat hypothalamus. J Comp Neurol. 1988; 274:60–76. [PubMed: 2458397]

Dehmel S, Cui YL, Shore SE. Cross-modal interactions of auditory and somatic inputs in the brainstem and midbrain and their imbalance in tinnitus and deafness. Am J Audiol. 2008; 17:S193–S209. [PubMed: 19056923]

Depuy SD, Kanbar R, Coates MB, Stornetta RL, Guyenet PG. Control of breathing by raphe obscurus serotonergic neurons in mice. J Neurosci. 2011; 31:1981–1990. [PubMed: 21307236]

Dun NJ, Dun SL, Forstermann U. Nitric oxide synthase immunoreactivity in rat pontine medullary neurons. Neurosci. 1994; 59:429–445.

Ellenberger HH, Feldman JL. Brainstem connections of the rostral ventral respiratory group of the rat. Brain Res. 1990; 513:35–42. [PubMed: 2350683]

Ennis M, Aston-Jones G, Shiekhattar R. Activation of locus coeruleus neurons by nucleus paragigantocellularis or noxious sensory stimulation is mediated by intracoerulear excitatory amino acid neurotransmission. Brain Res. 1992; 598:185–195. [PubMed: 1336704]

Ericsson A, Kovacs KJ, Sawchenko PE. A functional anatomical analysis of central pathways subserving the effects of interleukin-1 on stress-related neuroendocrine neurons. J Neurosci. 1994; 14:897–913. [PubMed: 8301368]

Feldman JL, Del Negro CA. Looking for inspiration: new perspectives on respiratory rhythm. Nat Rev Neurosci. 2006; 7:232–242. [PubMed: 16495944]

Feldman JL, Kam K, Janczewski WA. Practice makes perfect, even for breathing. Nat Neurosci. 2009; 12:961–963. [PubMed: 19636348]

Fenno L, Yizhar O, Deisseroth K. The development and application of optogenetics 23. Annu Rev Neurosci. 2011; 34:389–412. [PubMed: 21692661]

Fernandez de Sevilla D, Rodrigo-Angulo M, Nunez A, Buno W. Cholinergic modulation of synaptic transmission and postsynaptic excitability in the rat gracilis dorsal column nucleus. J Neurosci. 2006; 26:4015–4025. [PubMed: 16611818]

Fields HL, Heinricher MM, Mason P. Neurotransmitters in nociceptive modulatory circuits. Annu Rev Neurosci. 1991; 14:219–245. [PubMed: 1674413]

Fuller P, Sherman D, Pedersen NP, Saper CB, Lu J. Reassessment of the structural basis of the ascending arousal system 7. J Comp Neurol. 2011; 519:933–956. [PubMed: 21280045]

Gautron L, Lazarus M, Scott MM, Saper CB, Elmquist JK. Identifying the efferent projections of leptin-responsive neurons in the dorsomedial hypothalamus using a novel conditional tracing approach. J Comp Neurol. 2010; 518:2090–2108. [PubMed: 20394060]

Giuliano R, Ruggiero DA, Morrison S, Ernsberger P, Reis DJ. Cholinergic regulation of arterial pressure by the C1 area of the rostral ventrolateral medulla. J Neurosci. 1989; 9:923–942. [PubMed: 2926485]

Golanov EV, Ruggiero DA, Reis DJ. A brainstem area mediating cerebrovascular and EEG: responses to hypoxic excitation of rostral ventrolateral medulla in rat. J Physiol. 2000; 529:413–429. [PubMed: 11101651]

Gong S, Zheng C, Doughty ML, Losos K, Didkovsky N, Schambra UB, Nowak NJ, Joyner A, Leblanc G, Hatten ME, Heintz N. A gene expression atlas of the central nervous system based on bacterial artificial chromosomes. Nature. 2003; 425:917–925. [PubMed: 14586460]

Guyenet PG. The sympathetic control of blood pressure. Nat Rev Neurosci. 2006; 7:335–346. [PubMed: 16760914]

Guyenet PG, Bayliss DA, Mulkey DK, Stornetta RL, Moreira TS, Takakura AT. The retrotrapezoid nucleus and central chemoreception. Adv Exp Med Biol. 2008; 605:327–332. [PubMed: 18085294]

Guyenet, PG.; Stornetta, RL. The presympathetic cells of the rostral ventrolateral medulla (RVLM): anatomy, physiology and role in the control of circulation. In: Dun, NJ.; Machado, BH.; Pilowsky, PM., editors. Neural mechanisms of cardiovascular regulation. Kluwer Academic Publishers; Boston: 2004. p. 187-218.

Guyenet PG, Stornetta RL, Bayliss DA. Central respiratory chemoreception. J Comp Neurol. 2010; 518:3883–3906. [PubMed: 20737591]

Haselton JR, Guyenet PG. Ascending collaterals of medullary barosensitive neurons and C1 cells in rats. Am J Physiol-Reg Integr Comp Physiol. 1990; 258:R1051–R1063.

Hokfelt T, Fuxe K, Goldstein M, Johansson O. Immunohistochemical evidence for the existence of adrenaline neurons in the rat brain. Brain Res. 1974; 66:235–251.

Holmes CJ, Mainville LS, Jones BE. Distribution of cholinergic, GABAergic and serotonergic neurons in the medial medullary reticular formation and their projections studied by cytotoxic lesions in the cat. Neurosci. 1994; 62:1155–1178.

Huangfu D, Schreihofer AM, Guyenet PG. Effect of cholinergic agonists on bulbospinal C1 neurons in rats. Am J Physiol-Reg Integr Comp Physiol. 1997; 272:R249–R258.

Iadecola C, Faris PL, Hartman BK, Xu X. Localization of NADPH diaphorase in neurons of the rostral ventral medulla: possible role of nitric oxide in central autonomic regulation and oxygen chemoreception. Brain Res. 1993; 603:173–179. [PubMed: 8453473]

Ichikawa T, Ajiki K, Matsuura J, Misawa H. Localization of two cholinergic markers, choline acetyltransferase and vesicular acetylcholine transporter in the central nervous system of the rat: in situ hybridization histochemistry and immunohistochemistry. J Chem Neuroanat. 1997; 13:23–39. [PubMed: 9271193]

Jaarsma D, Ruigrok TJ, Caffe R, Cozzari C, Levey AI, Mugnaini E, Voogd J. Cholinergic innervation and receptors in the cerebellum. Prog Brain Res. 1997; 114:67–96. [PubMed: 9193139]

Jansen ASP, Wessendorf MW, Loewy AD. Transneuronal labeling of CNS neuropeptide and monoamine neurons after pseudorabies virus injections into the stellate ganglion. Brain Res. 1995; 683:1–24. [PubMed: 7552333]

Jensen P, Farago AF, Awatramani RB, Scott MM, Deneris ES, Dymecki SM. Redefining the serotonergic system by genetic lineage. Nat Neurosci. 2008; 11:417–419. [PubMed: 18344997]

Jones BE. Immunohistochemical study of choline acetyltransferase-immunoreactive processes and cells innervating the pontomedullary reticular formation in the rat. J Comp Neurol. 1990; 295:485–514. [PubMed: 2351765]

Kamiya H, Itoh K, Yasui Y, Ino T, Mizuno N. Somatosensory and auditory relay nucleus in the rostral part of the ventrolateral medulla: a morphological study in the cat. J Comp Neurol. 1988; 273(3): 421–435. [PubMed: 2463282]

Leong SK, Ling EA. Labelling neurons with fluorescent dyes administered via intravenous, subcutaneous or intraperitoneal route. J Neurosci Methods. 1990; 32:15–23. [PubMed: 2186224]

Li AJ, Wang Q, Dinh TT, Ritter S. Simultaneous silencing of Npy and Dbh expression in hindbrain A1/C1 catecholamine cells suppresses glucoprivic feeding. J Neurosci. 2009; 29:280–287. [PubMed: 19129404]

Loewy AD, Wallach JH, McKellar S. Efferent connections of the ventral medulla oblongata in the rat. Brain Research Rev. 1981; 3:63–80.

Lowell BB, Olson D, Yu J. Development and phenotype of ChAT-IRES-Cre mice. MGI Direct Data Submission. 2006 MGI Ref ID J:114556.

Lu J, Sherman D, Devor M, Saper CB. A putative flip-flop switch for control of REM sleep. Nature. 2006; 441:589–594. [PubMed: 16688184]

Maisky VA, Doroshenko NZ. Catecholamine projections to the spinal cord in the rat and their relationship to central cardiovascular neurons. J Auton Nerv Syst. 1991; 34(2-3):119–128. [PubMed: 1918805]

Morrison SF, Nakamura K, Madden CJ. Central control of thermogenesis in mammals. Exp Physiol. 2008; 93:773–797. [PubMed: 18469069]

Motts SD, Slusarczyk AS, Sowick CS, Schofield BR. Distribution of cholinergic cells in guinea pig brainstem. Neurosci. 2008; 154:186–195.

Nattie E, Li A. Central chemoreception is a complex system function that involves multiple brain stem sites. J Appl Physiol. 2009; 106:1464–1466. [PubMed: 18467549]

Okuda T, Haga T, Kanai Y, Endou H, Ishihara T, Katsura I. Identification and characterization of the high-affinity choline transporter. Nat Neurosci. 2000; 3:120–125. [PubMed: 10649566]

Padley JR, Kumar NN, Li Q, Nguyen TBV, Pilowsky PM, Goodchild AK. Central Command Regulation of Circulatory Function Mediated by Descending Pontine Cholinergic Inputs to Sympathoexcitatory Rostral Ventrolateral Medulla Neurons. Circulation Research. 2007; 100:284–291. [PubMed: 17204655]

Paxinos, G.; Franklin, KBJ. The Mouse Brain in Stereotaxic Coordinates. Elsevier; Amsterdam: 2004.

Ptak K, Yamanishi T, Aungst J, Milescu LS, Zhang R, Richerson GB, Smith JC. Raphe neurons stimulate respiratory circuit activity by multiple mechanisms via endogenously released serotonin and substance P. J Neurosci. 2009; 29:3720–3737. [PubMed: 19321769]

Punnen S, Willette RN, Krieger AJ, Sapru HN. Medullary pressor area: site of action of intravenous physostigmine. Brain Res. 1986; 382:178–184. [PubMed: 3768674]

Reis DJ, Morrison S, Ruggiero DA. The C1 area of the brainstem in tonic and reflex control of blood pressure. State of the art lecture. Hypertension. 1988; 11:I8–13. [PubMed: 3278978]

Rosin DL, Chang DA, Guyenet PG. Afferent and efferent connections of the rat retrotrapezoid nucleus. J Comp Neurol. 2006; 499:64–89. [PubMed: 16958085]

Ross CA, Armstrong DM, Ruggiero DA, Pickel VM, Joh TH, Reis DJ. Adrenaline neurons in the rostral ventrolateral medulla innervate thoracic spinal cord: a combined immunocytochemical and retrograde transport demonstration. Neurosci Lett. 1981; 25:257–262. [PubMed: 6270602]

Ross CA, Ruggiero DA, Joh TH, Park DH, Reis DJ. Adrenaline synthesizing neurons in the rostral ventrolateral medulla: a possible role in tonic vasomotor control. Brain Res. 1983; 273:356–361. [PubMed: 6616243]

Routledge C, Marsden CA. Adrenaline in the CNS: in vivo evidence for a functional pathway innervating the hypothalamus. Neuropharmacology. 1987; 26(7B):823–830. [PubMed: 2889157]

Ruggiero, DA.; Cravo, SL.; Arango, V.; Reis, DJ. Central control of the circulation by the rostral ventrolateral reticular nucleus: anatomical substrates. In: Ciriello, J.; Caverson, MM.; Polosa, C., editors. Progress in Brain Research, Vol. 81: The Central Neural Organization of Cardiovascular Control. Amsterdam; Elsevier: 1989. p. 49-79.

Ruggiero DA, Giuliano R, Anwar M, Stornetta R, Reis DJ. Anatomical substrates of cholinergic-autonomic regulation in the rat. J Comp Neurol. 1990; 292:1–53. [PubMed: 2312784]

Sawchenko PE, Li HY, Ericsson A. Circuits and mechanisms governing hypothalamic responses to stress: a tale of two paradigms. Progress in Brain Research. 2000; 122:61–78. [PubMed: 10737051]

Sawchenko PE, Swanson LW. The organization of noradrenergic pathways from the brainstem to the paraventricular and supraoptic nucleus in the rat. Brain Research Rev. 1982; 4:275–325.

Sawchenko PE, Swanson LW, Grzanna R, Howe PR, Bloom SR, Polak JM. Colocalization of neuropeptide Y immunoreactivity in brainstem catecholaminergic neurons that project to the paraventricular nucleus of the hypothalamus. J Comp Neurol. 1985; 241:138–153. [PubMed: 3840810]

Schreihofer AM, Guyenet PG. Baroactivated neurons with pulse-modulated activity in the rat caudal ventrolateral medulla express GAD67 mRNA. J Neurophysiol. 2003; 89:1265–1277. [PubMed: 12612005]

Shao XM, Tan W, Xiu J, Puskar N, Fonck C, Lester HA, Feldman JL. Alpha4* nicotinic receptors in preBotzinger complex mediate cholinergic/nicotinic modulation of respiratory rhythm. J Neurosci. 2008; 28:519–528. [PubMed: 18184794]

Smith JC, Abdala AP, Rybak IA, Paton JF. Structural and functional architecture of respiratory networks in the mammalian brainstem. Philos Trans R Soc Lond B Biol Sci. 2009; 364:2577–2587. [PubMed: 19651658]

Standish A, Enquist LW, Escardo JA, Schwaber JS. Central neuronal circuit innervating the rat heart defined by transneuronal transport of pseudorabies virus. J Neurosci. 1995; 15:1998–2012. [PubMed: 7891147]

Stocker SD, Steinbacher BC Jr. Balaban CD, Yates BJ. Connections of the caudal ventrolateral medullary reticular formation in the cat brainstem. Exp Brain Res. 1997; 116:270–282. [PubMed: 9348126]

Stornetta RL, McQuiston TJ, Guyenet PG. GABAergic and glycinergic presympathetic neurons of rat medulla oblongata identified by retrograde transport of pseudorabies virus and in situ hybridization. J Comp Neurol. 2004; 479:257–270. [PubMed: 15457502]

Swanson LW, Hartman BK. The central adrenergic system. An immunofluorescence study of the location of cell bodies and their efferent connections in the rat utilizing dopamine-beta-hydroxylase as a marker 80. J Comp Neurol. 1975; 163:467–505. [PubMed: 1100685]

Tan W, Pagliardini S, Yang P, Janczewski WA, Feldman JL. Projections of preBotzinger complex neurons in adult rats 13. J Comp Neurol. 2010; 518:1862–1878. [PubMed: 20235095]

Todd AJ. Neuronal circuitry for pain processing in the dorsal horn. Nat Rev Neurosci. 2010; 11:823–836. [PubMed: 21068766]

Tucker DC, Saper CB, Ruggiero DA, Reis DJ. Organization of central adrenergic pathways: I. Relationships of ventrolateral medullary projections to the hypothalamus and spinal cord. J Comp Neurol. 1987; 259:591–603. [PubMed: 2885348]

Veasey SC, Fornal CA, Metzler CW, Jacobs BL. Single-unit responses of serotonergic dorsal raphe neurons to specific motor challenges in freely moving cats. Neurosci. 1997; 79:161–169.

Wesselingh SL, Li YW, Blessing WW. PNMT-containing neurons in the rostral medulla oblongata (C1, C3 groups) are transneuronally labelled after injection of herpes simplex virus type 1 into the adrenal gland. Neurosci Lett. 1989; 106:99–104. [PubMed: 2555751]

Weston MC, Stornetta RL, Guyenet PG. Glutamatergic neuronal projections from the marginal layer of the rostral ventral medulla to the respiratory centers in rats. J Comp Neurol. 2004; 473:73–85. [PubMed: 15067719]

Whitsel BL, Petrucelli LM, Ha H, Dreyer DA. The resorting of spinal afferents as antecedent to the body representation in the postcentral gyrus. Brain Behav Evol. 1972; 5:303–341. [PubMed: 4629567]

Yasui Y, Cechetto DF, Saper CB. Evidence for a cholinergic projection from the pedunculopontine tegmental nucleus to the rostral ventrolateral medulla in the rat. Brain Res. 1990; 517:19–24. [PubMed: 2375988]

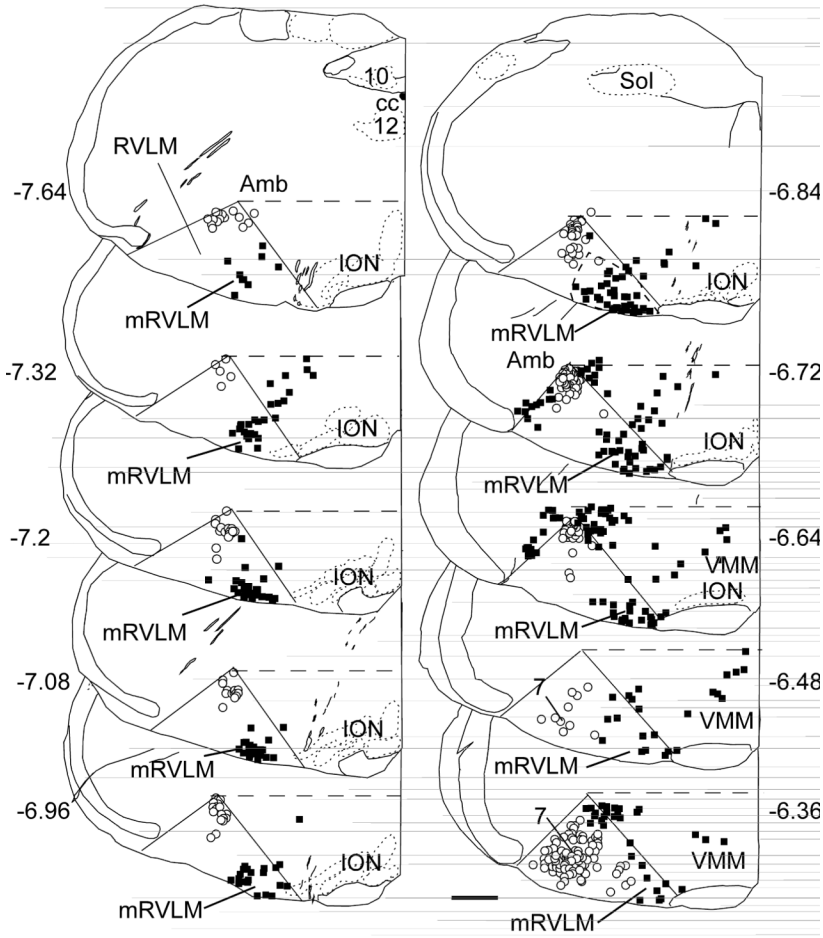

Fig. 1. Location of mRVLM cholinergic neurons in the mouse

Computer-assisted drawing of a series of 30-μm thick transverse sections through the rostral medulla of the mouse from the level of the obex forward. The numbers next to each section refer to their approximate level in mm behind bregma according to the mouse brain atlas of Paxinos and Franklin (2004). The rostral ventrolateral medulla (RVLM) is conventionally drawn in each section as a triangular area defined by nucleus ambiguus dorsally, the lateral edge of the pyramidal tract or inferior olive medially and the medial edge of the trigeminal tract laterally. The open circles represent ChAT-ir neurons labeled with Fluorogold (FG) after i.p. injection of this compound. These cells are either motor neurons or parasympathetic preganglionic neurons. The black squares represent ChAT-ir neurons without FG fluorescence, i.e. cholinergic neurons that do not project outside the brain. FG and ChAT-ir neurons located in the dorsal half of the medulla oblongata, i.e. above a horizontal line at the upper margin of nucleus ambiguus, are not represented in the plots. Note the dense cluster of ChAT-ir neurons at the lower right corner of the triangular RVLM region. This region is defined in this study as the mRVLM. *Scale bar* = 500 μm.

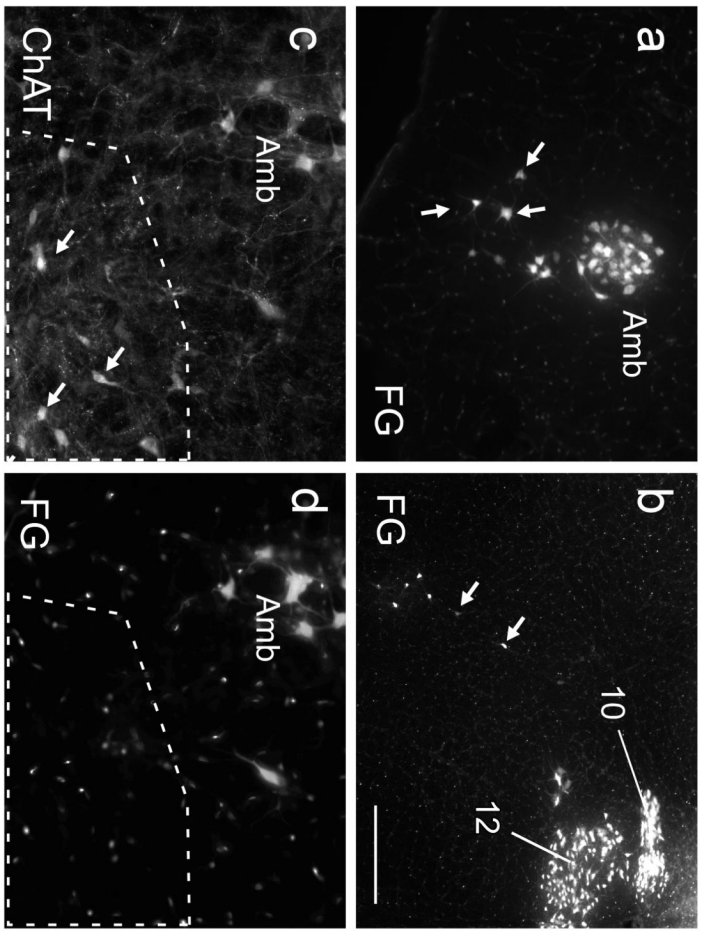

Fig. 2. The ChAT-ir neurons of the mRVLM are neither motor neurons nor parasympathetic neurons

a Fluorogold (FG) neurons within the compact subdivision of the ambiguus nucleus (Amb; left side of the brain) and surrounding reticular formation (loose formation of Amb.; arrows; approximate coronal level 6.6 mm caudal to bregma). FG natural fluorescence was visualized with an excitation filter of 365 nm and emission filter of 420 nm. These FG-labeled neurons are for the most part motor neurons that innervate the esophagus and airways and may include a few parasympathetic preganglionic neurons. **b** FG-labeled neurons within the dorsal medulla (obex level; left side of medulla oblongata). Hypoglossal nucleus (12) and dorsal motor nucleus of the vagus (10) are strongly labeled. Putative parasympathetic preganglionic neurons located within the intermediate reticular formation are indicated by arrows. **c,d** higher-power photographs of the mRVLM region (approximate bregma level −7.0 mm). **c** ChAT immunoreactivity visualized with Cy3 (excitation filter 545 nm, emission filter 605 nm). **d** FG illustrating the absence of FG in the mRVLM-ChAT-ir neurons (region outlined by the dotted line). ChAT-ir neurons belonging to the loose formation of the nucleus ambiguus can be seen dorsolaterally to the mRVLM. These neurons exit the CNS and contain FG as expected. *Scale bar* = 200 μm (**a,b**), 100 μm (**c,d**).

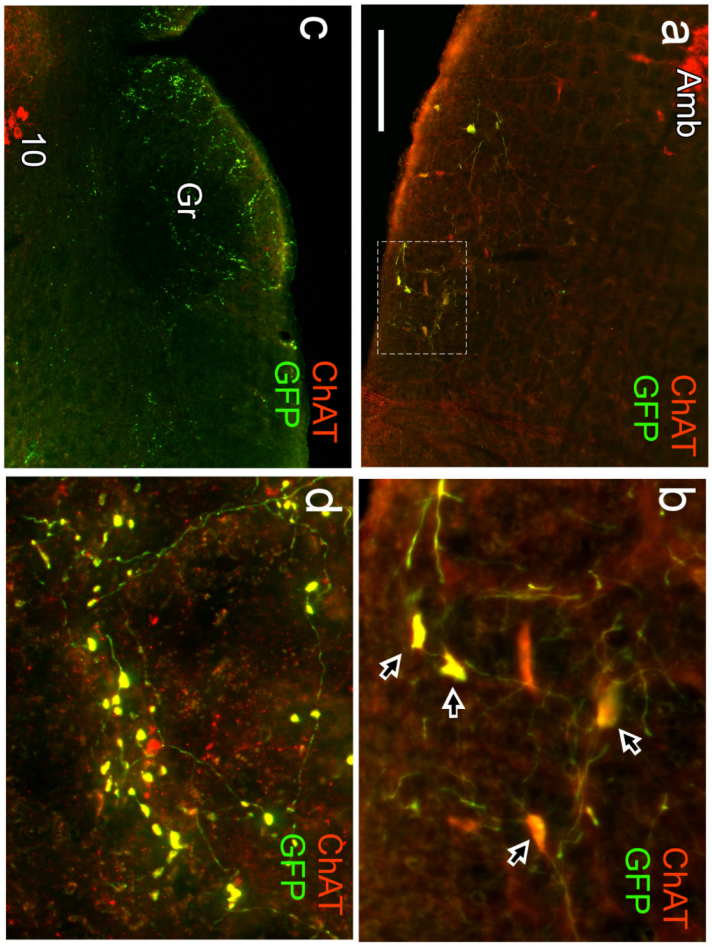

Fig. 3. Injection site and terminal field from one mouse injected with floxed-GFP-AAV2

a Injection site in a mouse in which floxed-GFP-AAV2 was introduced into the mRVLM. ChAT immunoreactivity is in red, GFP in green and neurons with both markers appear yellow. Transduced neurons are confined to the mRVLM. Note the lack of GFP in the compact portion of nucleus ambiguus (Amb) and in the large motor neurons of the loose formation of Amb. **b** higher power photograph of the area delineated in (**a)** by the dotted rectangle. Arrows point to neurons that express both GFP and ChAT-immunoreactivity (yellow). Note that all transduced neurons (GFP-positive) are ChAT-ir. **c,d** Examples of terminal fields observed in a mouse that received an injection of floxed-GFP-AAV2 in the mRVLM. **c** illustrates the contralateral gracile nucleus (Gr) and the surrounding region. The dorsal motor nucleus of the vagus (10) is visible at the lower left of the panel. **d** is a higher power photograph of gracile nucleus illustrating that all the GFP-labeled boutons are also ChAT-ir (these double-labeled boutons appear yellow). *Scale bar* = 200 μm (**a,c**) 50 μm (**b**), 20 μm (**d**).

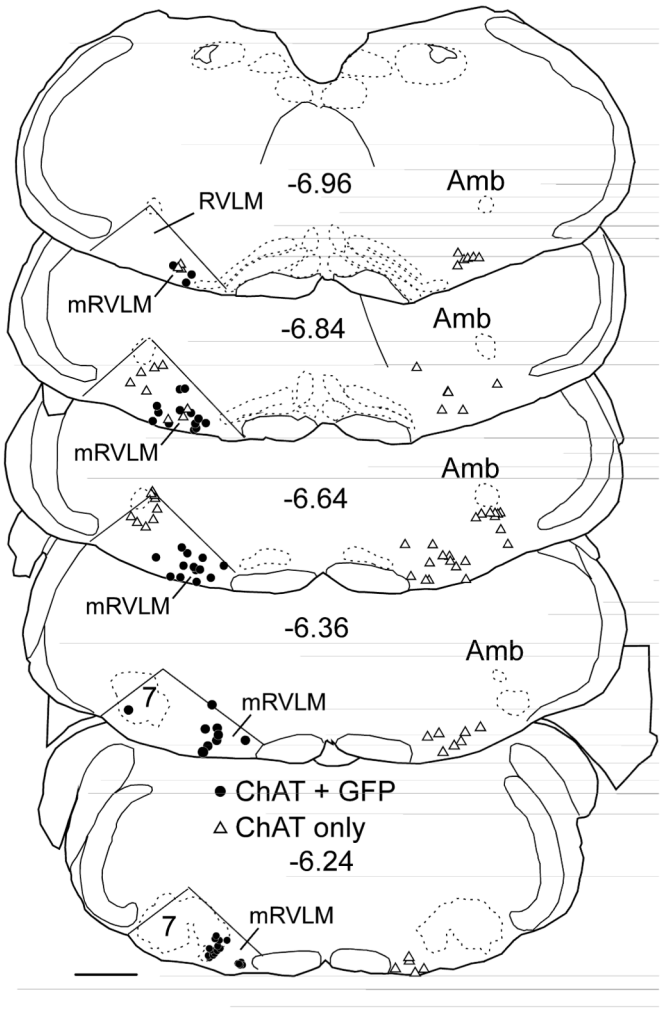

Fig. 4. Distribution of transduced ChAT neurons in case GFP3

In this case, we plotted only the ChAT-ir neurons located within the confines of the RVLM triangle defined in Fig. 1. Each circle indicates the location of a single ChAT-ir neuron that was transduced (i.e. GFP-ir). The triangles indicate the location of ChAT-ir neurons that were not GFP-positive. The ChAT-ir neurons located within the compact formation of the ambiguus (Amb) or within the facial motor nucleus (7) that were GFP-negative are not individually represented given their large numbers. This most favorable case is illustrated because it shows that under optimal conditions the vast majority of the RVLM ChAT-ir neurons were transduced suggesting that most of these neurons express Cre in the ChAT-Cre mouse used in this study. This example also illustrates a case in which a few facial motor neurons were transduced. Facial motor neurons exit the brain and presumably have few collaterals within the CNS. We therefore assumed that these neurons contributed little or not at all to the terminal fields described in this study. *Scale bar* = 500 μm.

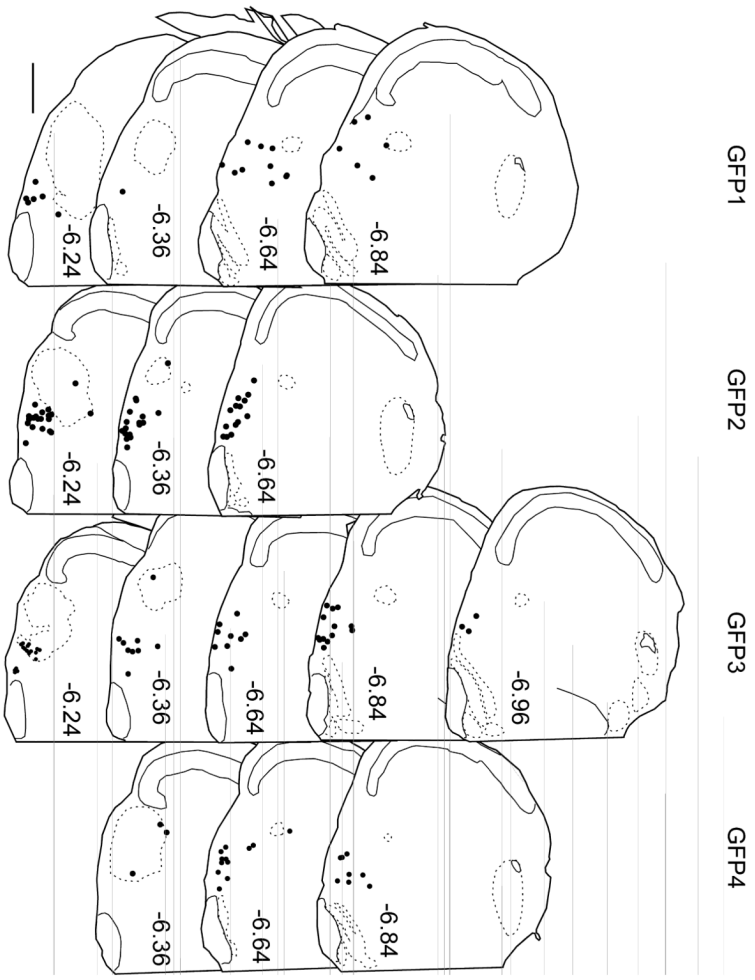

Fig. 5. Injection sites for all GFP-expressing AAV2 cases

Each dot represents the accurate (computer-assisted) location of a single cholinergic neuron labeled with GFP after injection of floxed-GFP-AAV2 into a ChAT-Cre mouse. Position relative to bregma (in mm) is noted to the left of each 30 μm-thick coronal section (after the atlas of Paxinos and Franklin (2004)). *Scale bar* = 500 μm.

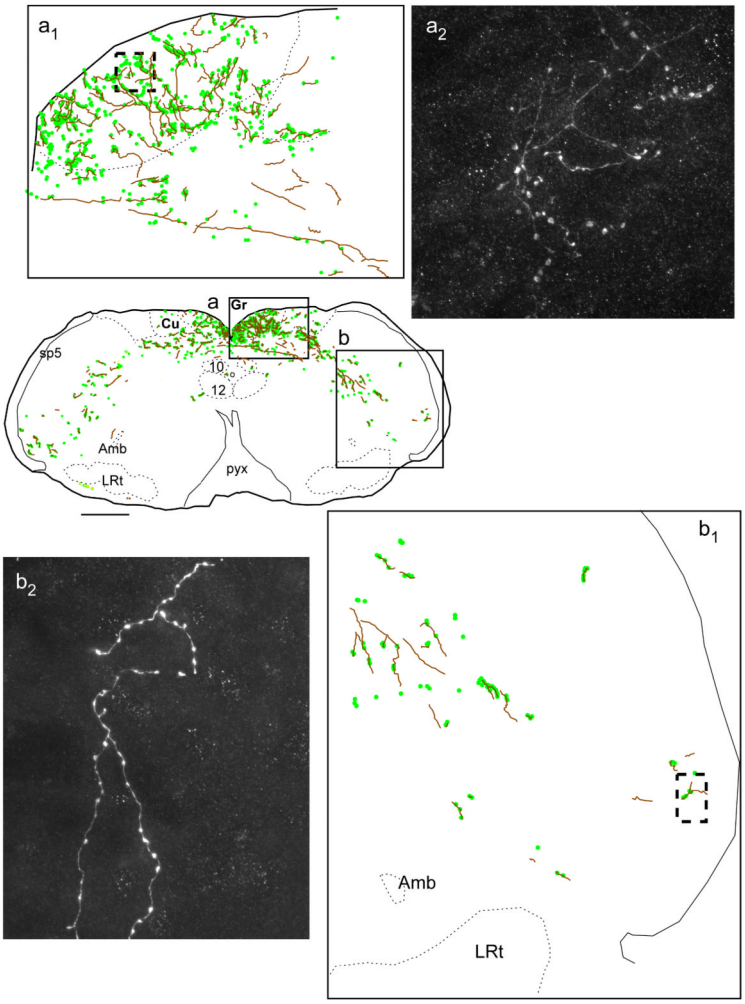

Fig.6. Injection sites for all mCherry-expressing AAV2 cases and overall distribution of transduced neurons in mRVLM of all cases

In the coronal brain maps, each dot represents the exact location of a single cholinergic neuron labeled with mCherry after injection of floxed-ChR2-mCherry-AAV2 into a ChAT-Cre mouse. Position relative to bregma (in mm) is noted to the left of each representative coronal section (after the atlas of Paxinos and Franklin (2004)). The graph below the brain maps shows the mean number of transduced ChAT neurons in the mRVLM at rostral to caudal levels indicated on the x axis as mm behind bregma of all mice injected with either the GFP vector (green circles –grey in print) or the mCherry vector (black squares) Note the similarity of the distribution of transduced neurons for both vectors. *Scale bar* = 500 μm.

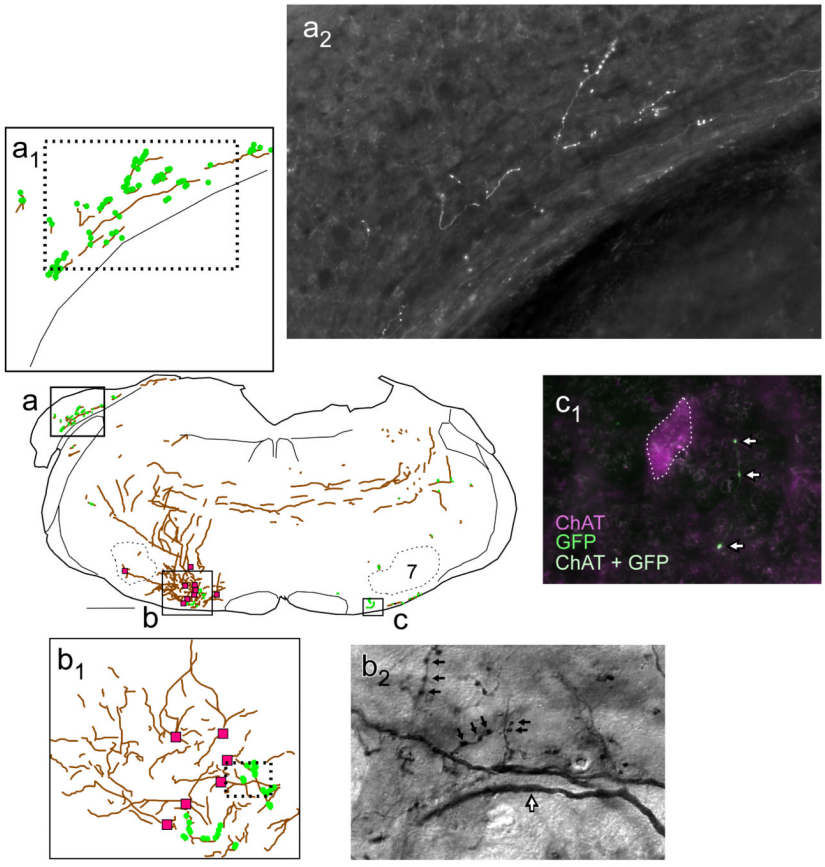

Fig. 7. Projections of mRVLM-ChAT neurons from case GFP3: dorsal column nuclei and spinal trigeminal nuclei

Axons are represented as gray lines (brown in online version). Small filled circles (green online) represent putative synaptic boutons labeled with GFP. The boxed region of the gracile nucleus shown in (**a)** is enlarged in (**a_1**) and a photomicrograph of the terminal field located within the dotted box in (**a_1**) is shown in (**a_2**). The portion of the trigeminal nucleus shown in (**b**) is enlarged in (**b_1**) and a photomicrograph of the region outlined by the dotted box in (**b_1**) is shown in (**b_2**) revealing fibers with varicosities. *Scale bar* = 500 μm (**a,b**), 100 μm (**a_1**), 125 μm (**b_1**), 12 μm (**a_2 ,b_2**).

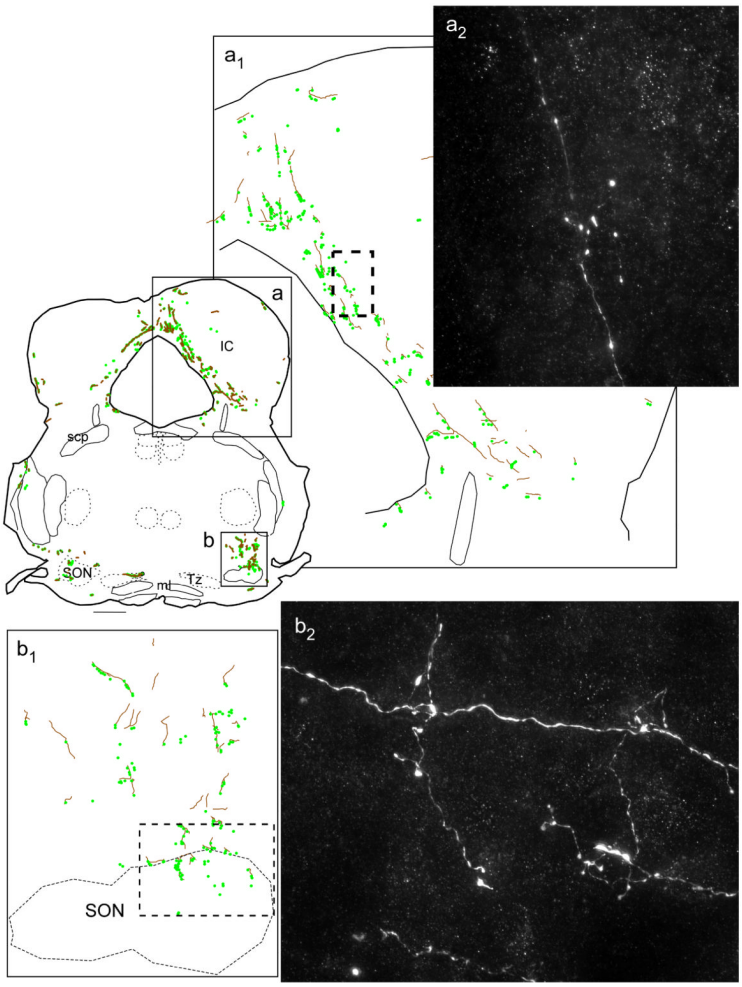

Fig. 8. Projections of mRVLM-ChAT neurons from case GFP3: dorsal cochlear nucleus, mRVLM and axonal decussation

Axons are represented as gray lines (brown in online version). Small filled circles (green online) represent putative synaptic boutons labeled with GFP. The region of the cochlear nucleus outlined in (**a**) is shown at higher magnification in (**a_1**). The region of the mRVLM outlined in (**b**) is shown at higher magnification in (**b_1**). In (**b)** and (**b_1**), the magenta squares represent mRVLM ChAT-ir neurons transduced with GFP. **b_2** is a photomicrograph of the region outlined by the dotted rectangle in (**b_1**). **b_2** illustrates the presence of GFP-ir putative synaptic boutons (small black arrows) and dendrites (black-rimmed white arrow) located in close proximity to the transduced mRVLM neurons. The contralateral mRVLM (**c**) also contained GFP-labeled cholinergic terminals as shown by the white arrows in (**c_1**). **c_1** shows the proximity of these terminals to a cholinergic neuron. *Scale bar* = 500 μm (**a-c**), 20 μm (**a_2**), 100 μm (**b_1**), 12 μm (**b_2**), 20 μm (**c_1**).

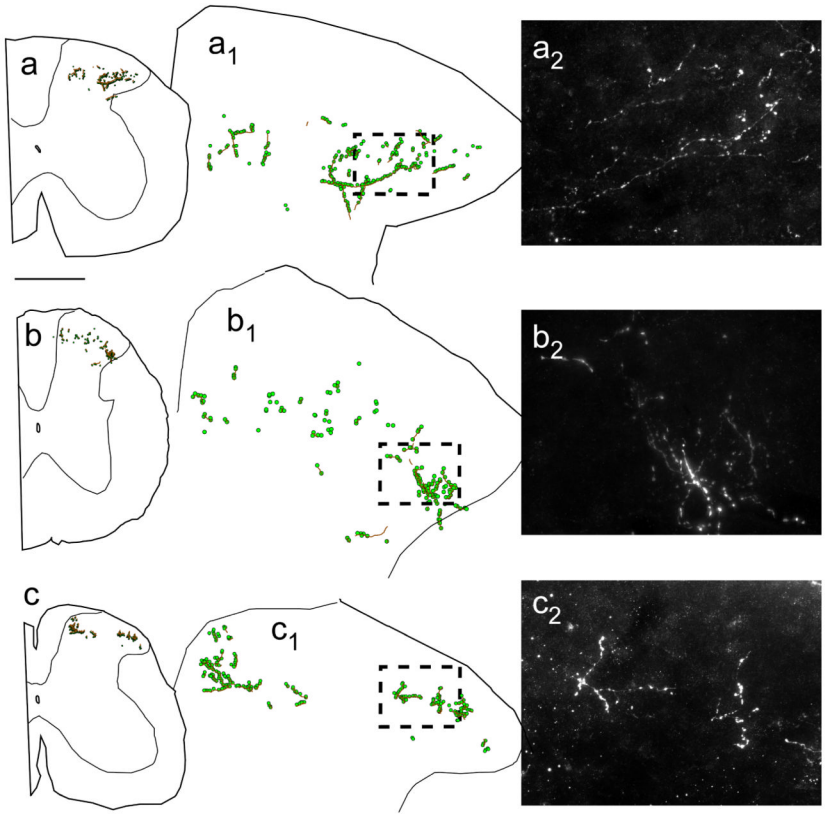

Fig. 9. Projections of mRVLM-ChAT neurons from case GFP3: periaqueductal gray, inferior colliculus (IC) and superior olivary nuclei (SON)

Axons are represented as gray lines (brown in online version). Small filled circles (green online) represent boutons labeled with GFP. The boxed region shown in the drawing (**a**) is enlarged in the drawing in (**a_1**) and a high power photomicrograph of the terminal field located within the dotted box in (**a_1**) is shown in (**a_2**). The region of the superior olivary complex outlined in (**b**) is enlarged in (**b_1**) and a high power photomicrograph of this region is shown in (**b_2**) revealing axons, axon bifurcations and varicosities. *Scale bar* = 500 μm (**a,b**), 150 μm (**a_1**), 83 μm (**b_1**), 10 μm (**a_2, b_2**).

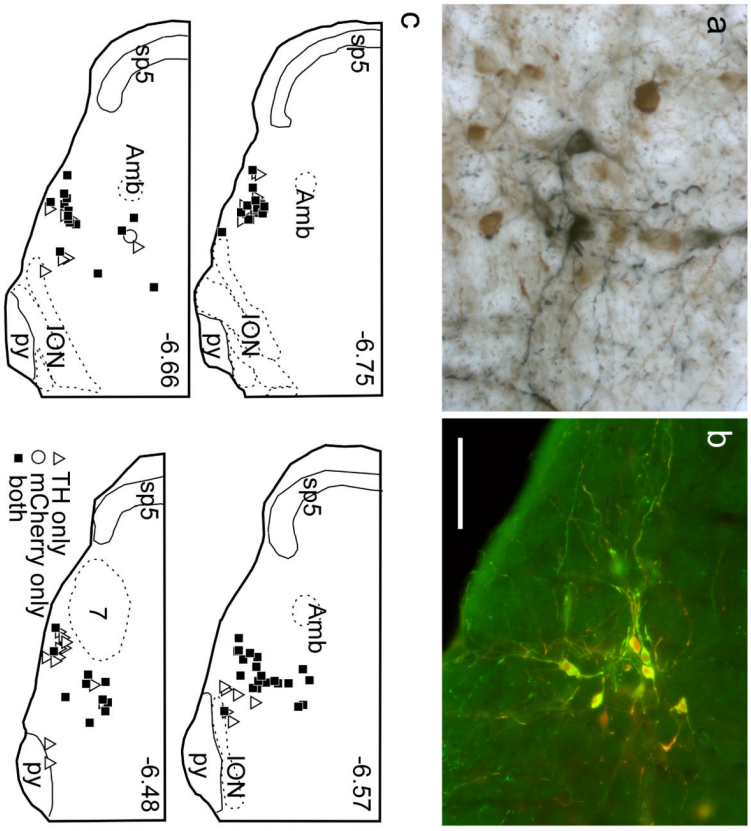

Fig. 10. Projections of mRVLM-ChAT neurons from case CR2: the spinal cord

Axons are represented as gray lines (brown in online version). Small filled circles (green online) represent boutons labeled with GFP. Projections were bilateral and targeted the same spinal cord regions. The contralateral densest projection is selectively illustrated in this figure. **a** cervical cord. **b** thoracic cord. **c** lumbar cord. **a_1, b_1, c_1** Enlargements of the dorsal horn regions illustrated in (**a**), (**b**) and (**c**). **a_2, b_2, c_2** Photomicrographs from the regions represented by the dashed boxes in (**a_1 - c_1**). *Scale bar* = 500 μm (**a- c**), 125 μm (**a_1- c_1**), 35 μm (**a_2- c_2**).

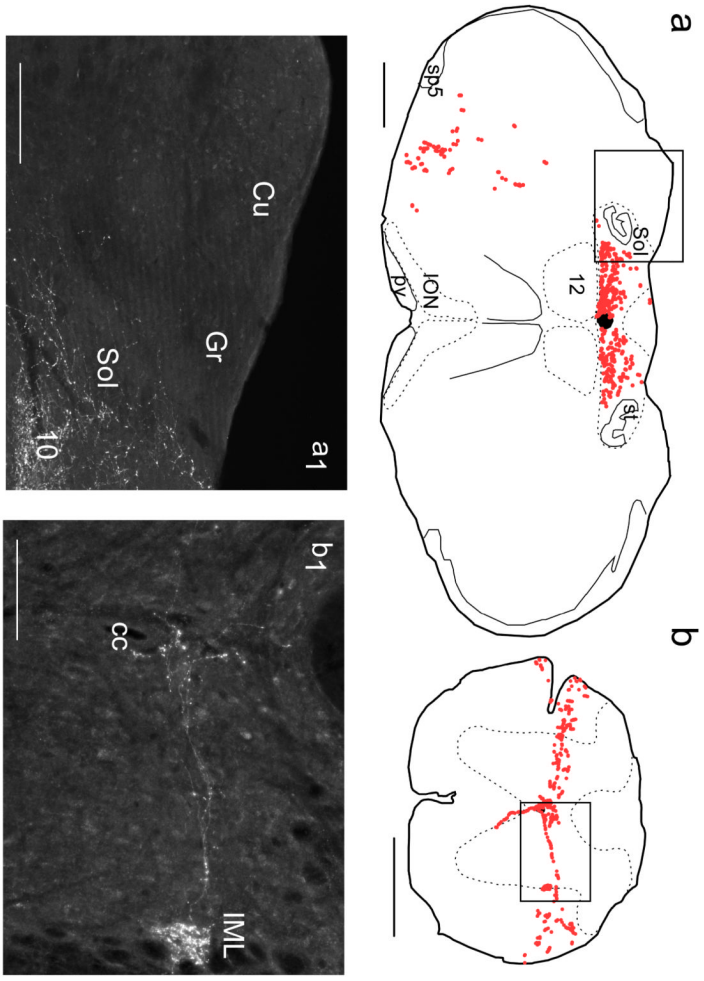

Fig. 11. Selective transduction of catecholaminergic neurons in the RVLM of the DBH-Cre mouse

a Photomicrograph illustrating the intermingling of tyrosine hydroxylase (TH)-ir and ChAT-ir neurons and processes within the mRVLM of a DBH-Cre mouse. ChAT-ir neurons and processes are brown and TH-ir neurons and processes are black. **b** Injection site three weeks after local microinjection of floxed-ChR2-mCherry-AAV2 into the RVLM of a DBH-Cre mouse. TH-immunoreactivity is in green and mCherry-immunoreactivity is red. All transduced neurons are also TH-ir and appear yellow. **c** Map of transduced neurons in one DBH-Cre mouse. Each square represents a single TH-ir neuron that was also mCherry-ir. Open triangles indicate TH-ir neurons devoid of mCherry immunoreactivity. Location of the section relative to bregma (in mm) is indicated in the upper right corner of each section (after Paxinos and Franklin (2004)). *Scale bar* = 50 μm (**a**), 100 μm (**b**), 500 μm (**c**).

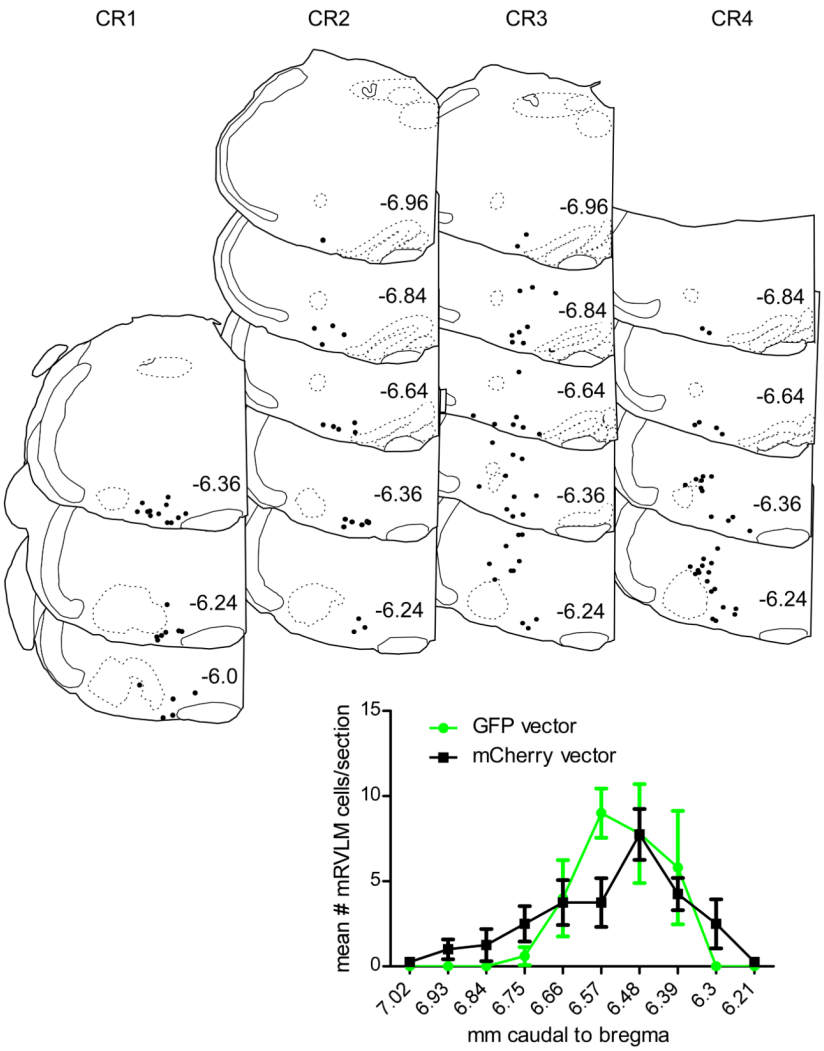

Fig. 12. Projections of RVLM catecholaminergic neurons: dorsomedial medulla and spinal cord

a Putative synaptic boutons (dots) identified in a 30 μm-thick transverse sections of the medulla oblongata at the level of the area postrema in a DBH-Cre mouse with floxed-ChR2mCherry AAV2 injected into the left RVLM. **a_1** Photomicrograph of the boxed region shown in (**a**). **b** Putative synaptic boutons identified in a transverse section of the thoracic spinal cord. **b_1** Photomicrograph of the boxed region drawn in (**b**). **a**, **a_1** The RVLM catecholaminergic neurons target the nucleus of the solitary tract (Sol) and dorsal motor nucleus of the vagus (10) but totally eschew the dorsal column nuclei (cuneate, Cu and gracile, Gr). **b**, **b_1** The catecholaminergic neurons of the RVLM target exclusively lamina X, the intermediolateral (IML) and intermediomedial cell column around the central canal (cc) but lack projections to the dorsal horn. *Scale bar* = 500 μm (**a,b**), 100 μm (**a_1, b_1**).

Brain Struct Funct. Author manuscript; available in PMC 2014 March 01.

Table

Summary of projections from all cases listed from caudal to rostral areas. +, low density of terminals, ++ high density. /c, contralateral predominance. -, no projection. n/a, tissue not available.GFP 1-4, cases from ChAT-Cre mice injected with floxed-GFP-AAV2. CR1-4, cases from ChAT-Cre mice injected with floxed-ChR2mCherry-AAV2. DBH1-4, cases from DBH-Cre mice injected with floxed- ChR2mCherry-AAV2.
This Table emphasizes the most consistent and densest projections of the mRVLM ChAT neurons. It is also designed to highlight the lack of overlap between the projections of these cholinergic neurons and those of the co-mingled catecholaminergic neurons, thereby also illustrating the specificity of the tracing method that was used. The catecholaminergic neurons of the RVLM have innumerable other targets (locus coeruleus, multiple hypothalamic and thalamic nuclei, amygdala). These regions do not receive inputs from the mRVLM ChAT cells and are not listed in the Table.

	GFP 1	**GFP 2**	**GFP 3**	**GFP 4**	**CR 1**	**CR 2**	**CR 3**	**CR 4**	**DBH 1**	**DBH 2**	**DBH 3**	**DBH 4**
dorsal horn (layer III)	n/a	n/a	n/a	n/a	++/c	++/c	++/c	++/c	-	-	-	-
IML	n/a	n/a	n/a	n/a	-	-	-	-	++	++	++	++
Gr	++	++/c	+	+	+	+	++/c	+	-	-	-	-
Cu	+	+	+	+	+	++	+	++	-	-	-	-
10	-	-	-	-	-	-	-	-	++	++	++	++
Sp5C	++/c	+	+	+	+/c	++/c	+/c	++/c	-	-	-	-
Sp5I	-	+	-	-	-	-	-	-	-	-	-	-
Sp5DM	+	+	+	+	+	+	++/c	+/c	-	-	-	-
Sol (lat)	-	+/c	+	+	+/c	+/c	+/c	-	-	-	-	-
Contra RVLM	+	+	+	+	+	+	+	+	+	+	+	+
SON	++/c	++	+	+/c	++/c	++	++	++/c	-	-	-	-
DC	+	+	+	+	+	+	+	+	-	-	-	-
Cerebellum	-	+	-	+	+	+	+	-	-	-	-	-
PAG	-	+/c	+	+	++	+	+	-	+	+	+	+
IC	-	+	+	-	+	+	+	-	-	-	-	-
dlPBN	-	-	+	-	+	-	+	+	++	++	++	++
LL nuclei	+	+	+	+	+	+	+	+	-	-	-	-